Chapter 2. Cation-π analysis using fluorinated Trp derivatives

2.1 Introduction

From the perspective of the participating molecules, the lock-and-key analogy for the binding of a neurotransmitter to its receptor is a rather optimistic description. In fact, the small molecule is tumbling, colliding with solvent molecules, spastically sampling different conformations as it diffuses through the medium. Upon entering the electrostatic field of its receptor, it's violently jerked this way and that by the protein's charged residues and hydrophobic cavities. Likewise, the multi-subunit receptor undergoes massive breathing motions on the timescale of the neurotransmitter's approach. Obtaining atomic-scale information about a binding event in the midst of this chaos is not easy. Everything depends on having a probe in the right place at the right time.

Classically, probe introduction has been accomplished in two rather different ways. Affinity labeling places the probe on the ligand and allows the receptor to position it accordingly. Any modification to the ligand which still allows binding may be introduced, including reactive groups for photoaffinity labeling, for example. The second means of obtaining structural information about ligand binding has been site-directed mutagenesis. The desirable aspect of this technique is the ability to precisely target single residues with discrete spatial locations. However, only the chemistry available to the natural amino acids may be utilized, such as disulfide formation using cysteine residues. As mentioned in the previous chapter, the extension of site-directed mutagenesis to accommodate synthetic amino acids has led to entirely new kinds of structural probes. For instance, a series of fluorinated tryptophan analogs has been used

in this laboratory as a sensitive probe of the role of side chain electrostatics in ligand binding.[1]

Ligand binding is a central event in almost every aspect of biology, and molecular neuroscience is no exception. The binding of small molecule neurotransmitters to membrane-bound receptors is the process which drives synaptic transmission. The advent of widespread cloning efforts in the past two decades or so has revealed the primary sequence of a large number of neurotransmitter receptors. Among the first of these was the nicotinic acetylcholine receptor (nAChR).[2] Attempts to understand the principles of molecular recognition by which the nAChR binds its agonist initially centered on attempting to reconcile the known amino acid sequence of the receptor with a variety of biochemical, electrophysiological, and pharmacological experiments, the conclusions of which have been extensively reviewed.[3-9] Muscle preparations and the electroplax organs of electric rays, which contain exceptionally dense clusters of nicotinic receptors, were used to conduct these experiments before advances in molecular biology made heterologous expression of the nAChR routine. Physiological experiments revealed that the nAChR is a cation channel which opens in response to acetylcholine, as well as nicotine. Furthermore, the apparent cooperativity of opening implied the presence of at least two agonist binding sites. Biochemical experiments involving photoaffinity labeling had identified a number of aromatic residues, both tyrosine and tryptophan, in the binding site. The observation that nAChR agonists are uniformly cationic had led to the expectation that anionic residues in the binding site would provide the necessary electrostatic attraction to draw neurotransmitters into the binding site.

However, it was also appreciated, particularly in this laboratory, that the aromatic residues identified by labeling studies could stabilize agonist binding through cation-π interactions.[10] Based on studies of molecular recognition of cationic substrates by synthetic hosts in water, the role of aromatic residues in binding acetylcholine was proposed in 1990.[11] In the absence of structural data on the nAChR, this proposal remained an attractive hypothesis until 1998, when the interaction was demonstrated directly.[1] In this set of experiments, the series of fluorinated Trp analogs alluded to above was introduced into the nAChR binding site by unnatural amino acid mutagenesis in *Xenopus* oocytes. At a single position in the binding site, a strict dependence on the negative electrostatic potential on the surface of the aromatic side chain was observed.[1] This dependence pointed to the role of Trp149 in ACh binding, via a cation-π interaction.

This assessment was subsequently confirmed in 2001 by the crystallization of a soluble acetylcholine-binding protein from the snail *Lymnaea helicalis*.[12] This crystallography represents a watershed event in structural analysis of ligand-gated ion channels, because the ACh binding protein (AChBP) is highly homologous to the extracellular portion of the nAChR. It is widely believed that structural insights gained from the AChBP crystal structure will be transferable to the extracellular domain of the receptor itself. One small detail of the crystal structure was quite gratifying to this laboratory. Cationic HEPES molecules from the crystallization buffer were reported to be bound to the face of the tryptophan homologous to the muscle Trp149 identified by Zhong *et al*. in 1998.[12]

Some of the structural detail revealed by the crystal structure is shown in Figure 2.1. Much of the gross structure had been previously gleaned from the physiological and

biochemical experiments mentioned above, along with primary sequence analysis and electron tomography.[9] The receptor is a pentamer, composed of five subunits around a central pore, which contains the ion channel region.

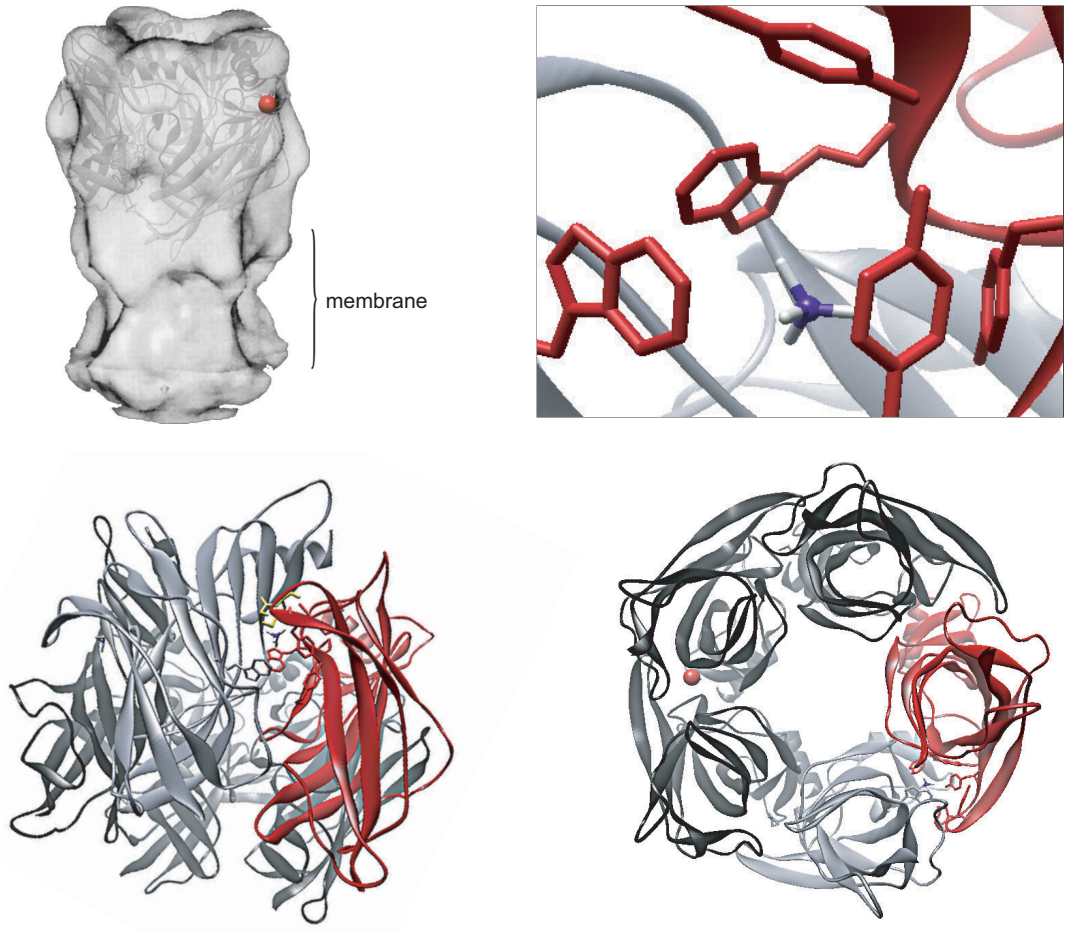

Figure 2.1 Views of the nAChR based on X-ray crystallography of the highly homologous snail acetylcholine binding protein.[12] Top left: Receptor electron density from electron cryomicroscopy,[9] superimposed over a ribbon diagram of AChBP, which corresponds to the extracellular domain of the receptor. Approximate location of bound agonist is indicated by the red sphere. Top right: Detailed view of the binding site, showing the arrangement of aromatic residues around the quaternary ammonium of the agonist. Bottom: Side and top views of the receptor with binding site residues in the subunit highlighted in red rendered as stick diagrams.

The muscle receptor is made up of four different subunits, denoted α, β, γ, and ε. The fetal form of the receptor, however, contains α, β, γ, and δ subunits, and it is this murine embryonic receptor used in the experiments below. In addition to the muscle-type receptor, found at neuromuscular junctions, there are neuronal forms of the receptor.[5,7,8]

Here, the subunit nomenclature differs somewhat. One class of subunits, which are identified by the presence of a vicinal Cys disulfide loop, is known as α. The muscle α is α1, and α2-9 are the neuronal isoforms. All other nicotinic subunits in the CNS are referred to as β, of which there are four known. Again, β1 is the muscle subunit and β2-4 are neuronal subunits.

The pore region of the nAChR is made up primarily of the second transmembrane region, known as M2. The conformational changes accompanying agonist binding are communicated to this transmembrane region, thus opening the channel. Previous work in this and other laboratories has identified mutations in the central region of this domain which confer greater sensitivity to agonists.[13-16] One of these mutations, Leu258Ser (also called L9'S, using commonly accepted nAChR nomenclature), will be utilized in the work below.

The binding domain, for which the structural information obtained from the AChBP applies, is the focus of the work presented below. The same series of fluorinated tryptophan analogs that was used to identify Trp149 as the cation-π binding site of ACh was employed to study the binding of a variety of agonists, revealing varying degrees of interaction with aromatic residues in the binding site. The behavior of nicotine was extensively characterized, along with a number of related nAChR agonist analogs. In addition, the technique was extended to a related serotonin receptor, the neuronal 5-HT_3R.[6,17] Unlike crystallography, this combination of unnatural amino acid mutagenesis and pharmacology is able to give information from only a single residue, so it lacks the scale of a crystal structure. However, it has the advantage over a crystal structure in that

it reports on the structure and function of residues in fully functioning ion channels in the plasma membrane of living cells.

2.2 Results

2.2.1 Nicotine dose-response to F_x-Trp at α149

The response of nAChR to nicotine was measured by two-electrode voltage clamp of oocytes expressing murine embryonic muscle nAChR. These receptors contained a pore mutation in the beta or gamma subunits, in order to reduce the EC_{50} and avoid channel block at higher agonist concentrations. Each L9'S mutation lowers EC_{50} by approximately a factor of ten relative to wild type. The effects of this mutation on EC_{50} are well-characterized, and it is expected not to alter agonist binding.[14,15,18] Dose-response curves for βL9'S receptors were collected by Wenge Zhong.[19] When a L9'S mutation is present in the β subunit, EC_{50} for otherwise wild-type nAChR is 45.3 ± 0.6 μM. If a single fluorine is added to the tryptophan ring by incorporating F-Trp at position 149, the EC_{50} rises to 129.8 ± 4.8 μM. This increase of almost threefold is comparable to the fourfold increase observed with ACh. What is observed, though, is that further fluorination does not lead to a significant further increase the EC_{50}. A small increase is noted for F_2-Trp, as the EC_{50} is 172.3 ± 5.7 μM. However, this is much smaller than the factor of four which characterizes the ACh interaction with Trp analogs at α149. Continuing in this vein, F_3-Trp gives an EC_{50} of 187.8 ± 11.4 μM and F_4-Trp produces a receptor with an EC_{50} of 136.4 ± 5.0 μM. Again, this increase is significantly less than that observed for ACh, implying that nicotine may not interact with Trp149 through a cation-π interaction.

The trend of these results was largely replicated in the receptor containing two L9'S mutations, as seen in Table 2.1. In this βγL9'S receptor, the EC_{50} for nicotine is 1.31 ± 0.45 μM. Introduction of F-Trp at position α149 causes a small increase to 4.19 ± 1.00 μM. However, further fluorination of the ring leads to little significant increase relative to the tenfold increase seen with acetylcholine. For F_2-Trp, the value is 5.43 ± 0.74 μM, increasing slightly to 12.56 ± 2.10 μM for F_3-Trp and to 10.93 for F_4-Trp.

L9'S	**Residue**	**EC_{50} (μM) SEM**	**n_H SEM**
β	Trp	45.3 ± 0.6	
β	F-Trp	129.8 ± 4.8	
β	F_2-Trp	172.3 ±5.7	
β	F_3-Trp	187.8 ± 11.4	
β	F_4-Trp	136.4 ± 5.0	
βγ	Trp	1.31 ± 0.32	2.92 ± 1.47
βγ	F-Trp	4.19 ± 0.71	1.57 ± 0.09
βγ	F_2-Trp	5.43 ± 0.52	1.53 ± 0.08
βγ	F_3-Trp	12.56 ± 1.49	1.13 ± 0.07
βγ	F_4-Trp	10.93	1.28

Table 2.1 Nicotine dose-response data for oocytes expressing β and βγ L9'S nAChR suppressed with the indicated residue at α149.

As an additional test that pore mutations exert their effects independently of binding interactions between agonists and Trp149, the response of ACh to fluorinated Trp analogs was measured in nAChR containing two L9'S mutation, in the beta and gamma subunits. (Table 2.2) These data replicate the trend observed for β L9'S by Zhong *et al.*[1,19]

Residue	**EC_{50} (μM)**	**n_H**
Trp	ND	ND
F-Trp	0.04	1.46
F_2-Trp	0.13	1.49
F_3-Trp	0.45	1.05
F_4-Trp	0.86	1.06

Table 2.2 ACh dose-response data for oocytes expressing βγ L9'S nAChR suppressed with the indicated residue at α149.

2.2.2 Nicotine dose-response to fluorination at other binding site Trp residues

The above results raise the question of how nicotine is binding to the receptor, if it does not rely on a cation-π interaction with Trp149. One possibility is that it retains the interaction, but with an aromatic residue other than Trp149. In order to test this hypothesis, a separate line of experimentation was undertaken involving probing other aromatic residues in the binding site for cation-π interactions. Initially, we focused on tryptophan residues implicated in nicotine binding by mutagenesis and photoaffinity labeling studies from other labs.[3-6] As in previous work with acetylcholine, these residues included αTrp86, αTrp184, γTrp55, and δTrp57. However, while this work was underway, the crystal structure of AChBP was published. From the crystal structure, it appears that of these four residues, only the γ55/δ57 pair are part of the agonist binding site around Trp149.[12] Because of this, only α184 and γ55/δ57 were tested.

The experimental procedure for this test was reported earlier.[1] In brief, 5-CN-Trp or 5-Br-Trp is incorporated into the receptor at the position of interest. Both these substituents withdraw electron density from the tryptophan ring, but the cyano group is much stronger in this regard than bromine, even though the two are similar in size. The calculated cation-π binding energy for 5-CN-Trp is 21.5 kcal/mol, relative to 27.8 kcal/mol for 5-Br-Trp. The expectation is that an agonist binding to the face of an aromatic ring at this position would be dramatically affected by the presence of 5-CN-Trp at this position and less by 5-Br-Trp. In the case of ACh at position 149, for example, there is an approximately 50-fold difference between 5-CN-Trp and 5-Br-Trp.[19] On the other hand, if binding to the face of an aromatic at this position is not important, little

difference between the two will be observed. At position α184, for instance, the ratio between 5-CN-Trp and 5-Br-Trp for ACh is 0.96.

As shown in Figure 2.2, nicotine shows no marked reliance on the aromatic face of side chains at α184 or γ55/δ57. At α184, the EC_{50} of receptors containing 5-CN-Trp is nearly identical to that of those containing 5-Br-Trp, which is no surprise if the AChBP structure reflects the actual structure of the nAChR binding site. At γ55/δ57, there is a slightly larger effect. EC_{50} for 5-CN-Trp is 1.43 ± 0.18 μM and 3.04 ± 0.45 μM for 5-Br-Trp. However, the ratio is approximately 0.5, well below that expected for an agonist relying on the energetics of a cation-π interaction for binding and, in fact, in the opposite direction.

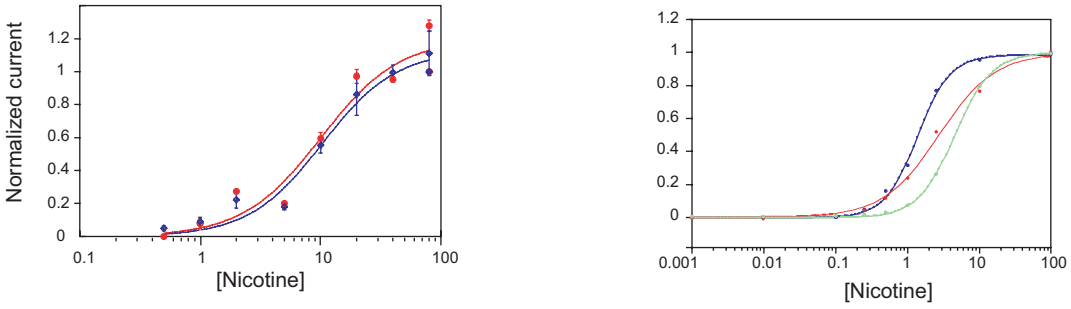

Figure 2.2 Nicotine dose-response for oocytes expressing nAChR suppressed at position α184 (left) and γ55/δ57 (right) with Trp (green), 5-CN-Trp (blue), and 5-Br-Trp (red). Receptors suppressed at α184 contain βγ L9'S mutations, while those suppressed at γ55/δ57 contain α L9'S.

From these data, we conclude that nicotine does not bind nAChR via a cation-π interaction at any of the sites tested. Most surprisingly, there is no apparent interaction with Trp149, at which cation-π interactions were observed for ACh and for serotonin at the homologous residue in the $5\text{-}HT_3R$. In light of photoaffinity labeling of γ55 by nicotine in experiments by Jonathan Cohen's lab, it is perhaps also surprising that the cation of nicotine does not apparently interact with γ55/δ57.[20,21]

2.2.3 N-methyl-nicotinium dose-response

One way in which protonated tertiary cations differ from quaternary cations is in their charge density and ability to benefit from cation-π interaction with aromatic systems. However, an equally important difference is that the protonated tertiary amine may lose its proton and revert to neutrality, presumably resulting in a non-binding form of the agonist. This is in contrast to the quaternary ammonium center, which is permanently charged under normal physiological conditions. In the case of nicotine, the pK_a of the pyrrolidinium nitrogen is 7.8, quite close to physiological pH.[22] Thus, it is quite reasonable to suppose that the microenvironment at the nAChR binding site might be sufficiently basic to induce deprotonation. Further, it is reasonable to suppose that perturbing the electrostatics of the side chain at α149 might alter the electrostatics of the binding site in such a way as to promote or hinder deprotonation. In order to test the hypothesis that fluorination affects not only the cation-π binding ability of the residue at α149 but also the protonation state of nicotine, a quaternary analog of nicotine, *N*-methyl-nicotinium, was prepared by Niki Zacharias.[22]

Sterically, *N*-methyl-nicotinium is bulkier than nicotine, as a result of the additional *N*-methyl group. As discussed, the relatively diffuse charge density decreases the ability of this quaternary cation to interact with the face of an aromatic residue relative to nicotine. Finally, the quaternary analog of nicotine is unable to undergo deprotonation and thus serves as a test for the hypothesis that fluorination at α149 promotes deprotonation and results in an apparent decrease in agonist affinity. As shown in Table 2.3, the EC_{50} for *N*-methyl-nicotinium in βγL9'S nAChR is 0.77 ± 0.14 μM, quite similar to that that of nicotine. (Table 2.1) In response to F-Trp, the EC_{50} increases fivefold to

4.23 ± 0.44 μM. Like nicotine, *N*-methyl-nicotinium does not respond significantly to further increases in fluorination. F_2-Trp gives rise to an EC_{50} of 5.70 ± 0.76 μM, F_3-Trp to 3.27 ± 0.44 μM, and F_4-Trp to 4.56 ± 1.01 μM. Thus, it seems that changes in protonation state do not account for the increased EC_{50} of F_x-Trp. Furthermore, quaternized nicotine does not appear to acquire a cation-π interaction.

Residue	EC_{50} (μM)	SEM	n_H	SEM
Trp	0.77 ± 0.14		1.34	± 0.07
F-Trp	4.23 ± 0.44		1.44	± 0.08
F_2-Trp	5.70 ± 0.76		1.42	± 0.09
F_3-Trp	3.27 ± 0.44		1.33	± 0.07
F_4-Trp	4.56 ± 1.01		1.05	± 0.13

Table 2.3 *N*-methylnicotinium dose-response data for oocytes expressing βγ L9'S nAChR suppressed with the indicated residue at α149.

2.2.4 Noracetylcholine dose-response

A complementary line of experimentation analyzed the behavior of a tertiary analog of ACh. The expectation, strictly on charge-density considerations, is that this agonist should show a steeper slope in the plot of EC_{50} versus cation-π binding ability of α149. However, the data do not conform to this expectation (Table 2.4).

Residue	EC_{50} (μM)	SEM	n_H	SEM
Trp	22.75 ± 6.45		2.62 ± 1.00	
F-Trp	161.03 ± 9.31		1.92 ± 0.26	
F_2-Trp	225.46 ± 27.92		1.62 ± 0.04	
F_3-Trp	326.59 ± 18.16		1.62 ± 0.03	
F_4-Trp	152.24 ± 4.31		1.53 ± 0.03	

Table 2.4 NorACh dose-response data for oocytes expressing βγ L9'S nAChR suppressed with the indicated residue at α149.

Noracetylcholine is vastly inferior to the natural agonist, with an EC_{50} of 22.75 ± 6.45 μM in the βγL9'S receptor. Interestingly, the tertiary analog of ACh shows a trend which is ambiguous as to whether or not it implies a cation-π interaction with α149. The EC_{50} for norACh in receptors containing F-Trp is 161.03 ± 9.31 μM, a sevenfold increase. However, EC_{50} with F_2-Trp at α149 is 225.46 ± 27.92 μM, F_3-Trp is

326.59 ± 18.16 μM, and F_4-Trp is 152.24 ± 4.31 μM. As with nicotine, there is a formal possibility that norACh is being deprotonated in the binding site, although the pK_a of this amine is greater (8.3).[23]

2.2.5 Variation of pH with tertiary ACh

Work by James Petersson in this laboratory has shown that the apparent local pK_a of amine-containing compounds in the muscle receptor binding site differs dramatically from their behavior in bulk solvent.[24] We reasoned that it may be such a distinction which accounts for the marked difference in response to ACh and the very similar compound norACh. To provide an initial test of this hypothesis, the trend of activation by norACh with varying pH was investigated. (Figure 2.3)

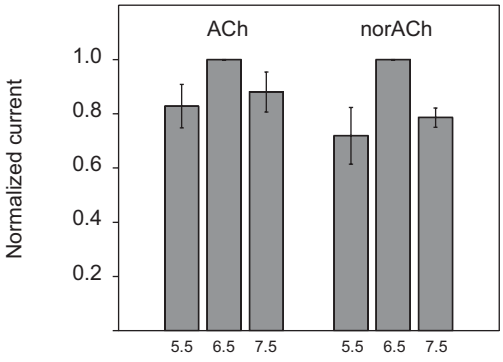

Figure 2.3 ACh and norACh response in αL9'S muscle nAChR measured at varying pH. Mean whole-cell currents were recorded in response to 10 μM ACh and 100 μM norACh, then normalized to the maximal current and are reported as the mean value (±SEM).

The whole-cell current peaked at pH 7.5 for both agonists, and no great difference was observed between the behavior of tertiary and quaternary analogs. It may be that the binding-site environment shields agonists from buffer pH effects, but the lack of overt variation with pH is perhaps suggestive that the potential proton lability of norACh does not account for the difference between its behavior and that of ACh.

2.2.6 TMA dose-response

It also appears that weak agonism does not necessarily correlate with lack of a cation-π interaction with α149, since data for TMA reported by Wenge Zhong show the expected trend for cation-π interactions.[19] Here, the EC_{50} for βδL9'S nAChR is 47.6 ± 1.7 μM, comparable to that of norACh. There is a significant increase with F-Trp, to 155.4 ± 3.5 μM, and additional linear increase to 312.7 ± 8.0 μM for F_2-Trp and 788.6 ± 22.7 μM for F_3-Trp. Thus, the absence of a cation-π interaction between norACh and α149 cannot be explained by the low efficacy of norACh relative to ACh. Nor is it the case that cation-π interactions are only observed with quaternary agonists, as primary and secondary serotonin analogs undergo the interaction with the 5-HT_3 receptor.

2.2.7 Serotonin binding to 5-HT_{3A}R substituted with F_x-Trp series at W183

The position in the 5-HT_{3A}R homologous to α149 in the mouse muscle receptor was substituted with the series of fluorinated Trp analogs. The results for W183 suppression were obtained by Darren Beene and are reported in Table 2.5. As was observed for the nAChR, the other Trp side chain which aligns with the conserved residues of the aromatic box was tested and showed no difference between Trp and F_4-Trp. Thus, it appears that the behavior of residue 183 is unique.

2.2.8 Binding of tertiary and quaternary 5-HT analogs

In an effort to understand whether ammonium centers with differing degrees of alkylation, such as those of nicotine and ACh, interact more or less strongly with aromatic residues, a series of *N*-alkylated serotonin analogs was tested on the 5-HT_{3A}R.

In the usual fashion, the series of fluorinated Trp analogs was incorporated at position 183 and dose-response relations collected. (Table 2.5)

2.2.9 Involvement of hydrogen bonding at W183 investigated

As in the case of the initial studies on the nAChR carried out by Wenge Zhong, we were mindful of the fact that fluorination of the tryptophan side chain changes the hydrogen bond donation ability of the indole nitrogen as well as the electrostatic character of the aromatic portion of the molecule.[1] As before, in order to verify that the observed effects were not due to hydrogen bonding, a series of non-hydrogen bonding analogs of tryptophan with similar calculated cation-π binding energy was tested at position 183 by Darren Beene. The results of these experiments are also reported in Table 2.5.

Residue	EC_{50}±SEM (μM)	Hill coefficient±SEM
5-HT		
Trp	1.21±0.06	2.0±0.16
F-Trp	6.03±0.51	1.4±0.14
F_2-Trp	37.7±2.96	1.9±0.23
F_3-Trp	244±8.4	2.5±0.17
***N*-Me-5-HT**		
Trp	1.82±0.10	2.5±0.13
F-Trp	2.70±0.17	1.9±0.19
F_2-Trp	23.1±2.73	2.6±0.22
F_3-Trp	368±	2.0±0.10
5-HTQ		
Trp	1.07±0.07	2.1±0.25
F-Trp	1.65±0.15	1.65±0.19
F_2-Trp	12.8±0.95	1.8±0.19
F_3-Trp	284±18.7	2.0±0.15
5-HT		
1-Nap-Ala	30.4±1.75	1.6±0.10
2-Nap-Ala	32.0±2.30	1.6±0.12
N-Me-Trp	25.6±1.66	1.8±0.16
Trp 90		
Trp	1.21±0.06	2.0±0.16
F_4-Trp	1.01±0.049	1.6±0.09

Table 2.5 Serotonin and 5-HT analog dose-response data for oocytes expressing $5-HT_{3A}R$ suppressed with the indicated residue at position 183 and, where indicated, 90.

2.2.10 Efficacy

The EC_{50} for a receptor is a composite measurement, comprising multiple elementary steps. Even in the most simplistic two-state model of channel opening, agonist binding to the closed channel is followed by a conformational change to an open channel state. Since the dose-response measurement fails to deconvolute these two steps, experiments were undertaken to determine whether binding or channel gating accounted for the observed alterations in EC_{50} in response to increasing Trp fluorination. The efficacy of a compound on a ligand-gated ion channel is reflected in the maximal current passed at saturating agonist concentration under given electrophysiological conditions.[25,26] Relative efficacies of all nicotinic drugs were determined in ND96 medium in oocytes clamped at a membrane potential of -80 mV at a concentration approximately five times the EC_{50} of the compound. (Figure 2.4)

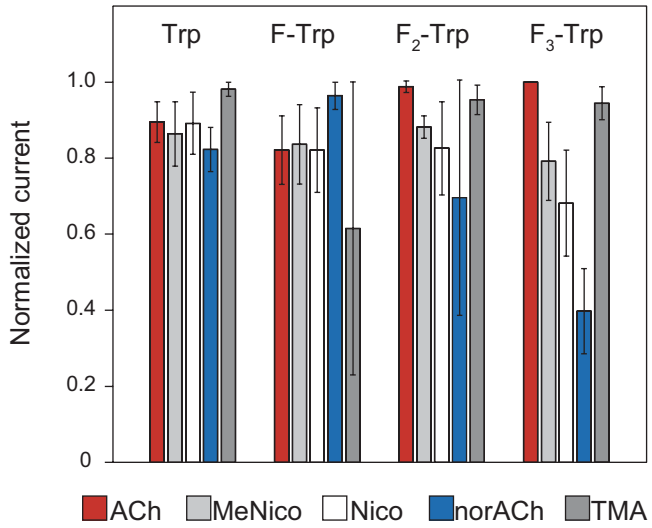

Figure 2.4 Efficacy measurements for oocytes expressing βγ L9'S nAChR suppressed with the indicated residue at α149ACh, in response to saturating concentrations of the indicated agonist. Mean whole-cell currents were obtained and normalized to the maximal signal elicited for each oocyte. Normalized data were averaged and are reported along with SEM. Concentrations of each agonist were ACh, 10 and 100 μM; *N*-Me-nicotinium, 10 and 100 μM; nicotine, 10 and 100 μM; norACh, 100 and 500 μM; and TMA, 250 and 500 μM.

For the nAChR agonists considered here, there was no significant difference in efficacy among them. Nor was the relative efficacy observed to differ in receptors containing fluorinated Trp analogs. There are some small effects, such as the apparent drop in efficacy of TMA with F-Trp and norACh with F_3-Trp, although in both cases the sample size was small and at least one oocyte showed uniform efficacy for all five compounds. Also, the measurements were taken at high concentrations, in order to obtain maximal current. Particularly with fluorinated Trp residues, the potency of certain compounds is sufficiently low that maximally efficacious concentrations begin to overlap with concentrations which induce channel block. Data for TMA and norACh were particularly affected. Additional data were collected at -40 mV, in an attempt to reduce open-channel block by these agonists, although it differed little from that collected at -80 mV.

The process of channel gating is a complicated one and is postulated to involve numerous elementary steps for the nAChR. Thus, it is overly simplistic to conclude from these efficacy experiments that the effects observed are due exclusively to binding.[27] However, the fact that all compounds tested exhibit the same efficacy is somewhat suggestive that the effects we observe are primarily relevant to binding. The ability of these compounds to initiate the conformational changes associated with channel opening is not apparently affected by the presence of variously fluorinated Trp analogs in the binding site. Thus, the large effects that we see on potency probably arise due to effects on agonist binding.

2.2.11 Results from neuronal nAChR

Unlike the muscle-type nAChR, neuronal nicotinic receptors uniformly show higher affinity for nicotine than they do for ACh.[5] It would be quite interesting to know whether these high-affinity nicotine receptors bind nicotine via a cation-π interaction with the Trp149 homolog, which is conserved across all nAChR. However, these receptors proved not to be amenable to unnatural amino acid suppression. Wild-type recovery in the α4β2 receptor was possible, although injection of 25 ng of total mRNA in various subunit ratios gave rise only to several hundred nA of whole-cell current at -80 mV in ND96 under the most optimal circumstances. Fluorinated analogs expressed even more poorly, with less than 100 nA whole-cell current. As a result, dose-response curves could not be collected for α4β2 receptors. Chimeric constructs consisting of the extracellular domain of neuronal nAChR α4, β2, and α7 and the transmembrane domains of the 5-HT_3R have been shown to express better than native nAChR in numerous cell lines.[28-32] These constructs also failed to give substantial currents in wild-type recovery suppression experiments. Work to increase the expression efficiency of neuronal receptors in nonsense suppression experiments in *Xenopus* oocytes is treated in further detail in Section 2.4.

2.3 Discussion

The binding of a neurotransmitter to its receptor is a testament to the organizing power of weak, noncovalent interactions. Determining the impact these low-energy interactions have on a dynamic process such as molecular recognition requires that the analysis, involving physical organic chemistry, be carried out on a functioning integral membrane protein. The technique of introducing synthetic amino acid side chains

through *in vivo* nonsense suppression is one of the few methods available for performing such analyses. In the case of the nicotinic acetylcholine receptor, we have previously proposed a unique role for Trp149 in the alpha subunit in the binding of the natural agonist, acetylcholine.[1] The cation-π binding ability of the side chain at this position was subtly and serially altered by introducing a series of increasingly fluorinated tryptophan derivatives.[33,34] (Figure 2.5)

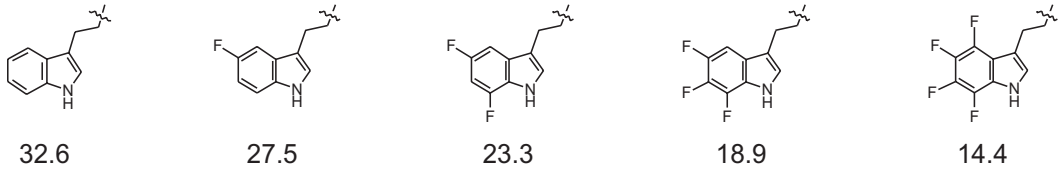

Figure 2.5 The series of fluorinated Trp analogues, with the gas phase cation-π binding energy of fluoroindoles (HF 6-31G**) in kcal/mol.[33,34]

The ability of ACh to trigger receptor opening decreased with decreasing cation-π binding ability of the side chain at this position. From this, we concluded that α149 participated in a direct cation-π interaction with the quaternary ammonium center of ACh. More recent structural work from other labs has confirmed our conclusion and provided much greater detail as to the composition of the binding site.[12] (Figure 2.6 and Figure 2.7)

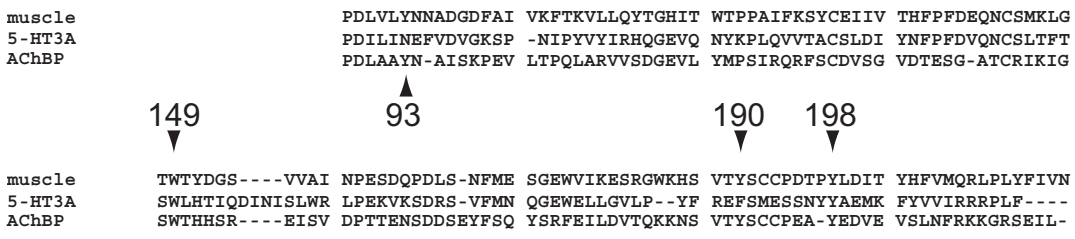

Figure 2.6 Sequence alignment of muscle nAChRα, 5-HT_{3A}R, and AChBP.[12,35,36] The residues which comprise the aromatic box are indicated with arrows, with the exception of the Trp residue contributed by the interfacial subunit, which is conserved among all members of the nAChR receptor family and which is γ55 or δ57 in muscle nAChR.

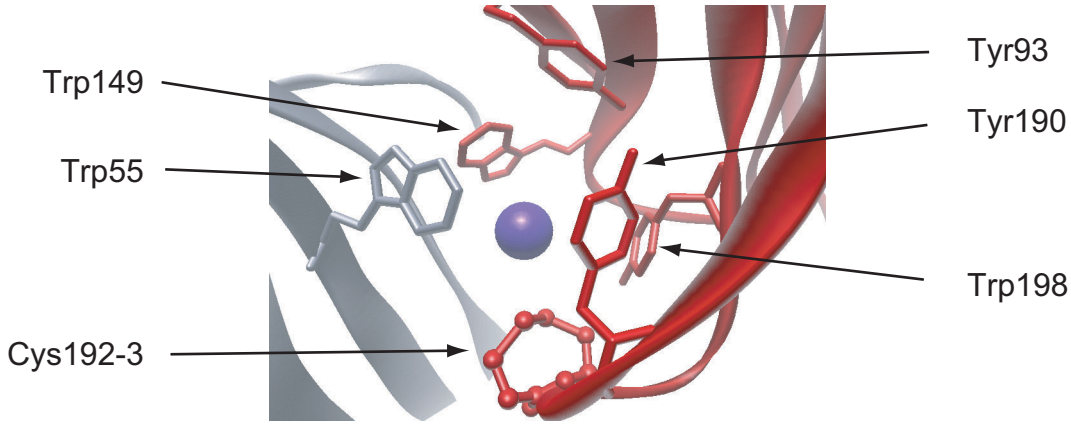

Figure 2.7 Diffraction data from AChBP showing the quaternary ammonium center (blue) of a HEPES molecule from the crystallization buffer bound to the face of Trp143, the homolog of muscle nAChR Trp149 and 5-HT_{3A}R Trp183. The residues of the aromatic box comprising the nAChR active site are numbered according to the nAChR muscle numbering. Trp55 is from the γ subunit.

In the work presented here, we extend this technique to consider the binding of the pharmacologically important nAChR agonist, nicotine. In addition, the approach of altering side chain electrostatics is complemented by modification of the ammonium center of both ACh and nicotine. Finally, related work by Beene on the ligand-gated serotonin receptor, 5-HT_3R, is introduced to support and further the analysis of results obtained on the nAChR.

2.3.1 Anomalous behavior of nicotine

Probing nAChR containing variously fluorinated Trp derivatives with ACh gives a very clear relationship between calculated cation-π binding energy and the measured dose-response.[1] However, this is not true at all with nicotine.[19] As may be appreciated from Figure 2.8, fluorination of Trp149 gives rise to a receptor with diminished responsiveness to nicotine. However, further fluorination does not further impact nicotine's ability to open the channel. Thus, it does not appear that there is a direct electrostatic interaction between the ammonium center of nicotine and Trp149. Nicotine

is a full agonist for the nAChR and would be expected by all conventional pharmacophore models to share roughly the same binding mode as ACh.[37-42]

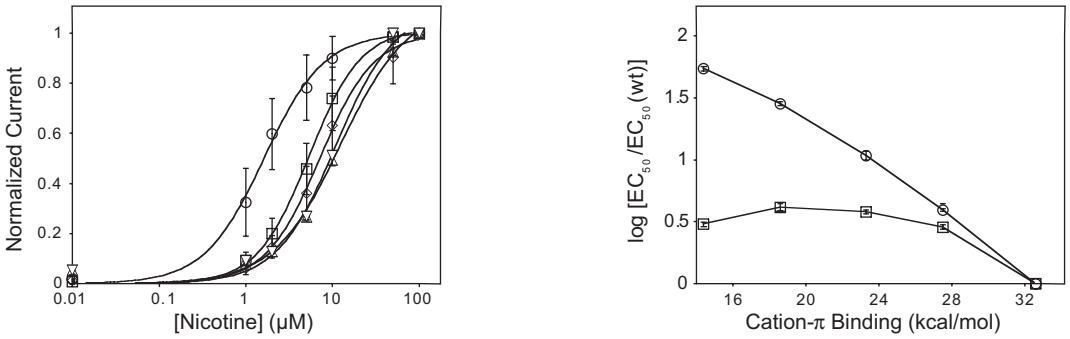

Figure 2.8 Electrophysiological analysis of nicotine. Left panel: Nicotine dose-response relations for βγ L9'S nAChR suppressed with Trp (O), F-Trp (□), F_2-Trp (◊), F_3-Trp (△), and F_4-Trp (▽) at α149. (b) Fluorination plot for ACh (O) and nicotine (□) at the nAChR.

2.3.2 Similarity between ACh and serotonin

The linear response to fluorination seen with ACh is not a property peculiar to the nAChR. The introduction of a series of fluorinated Trp analogs at position 183 of human 5-HT_3R provides clear evidence for a cation-π interaction between this residue and serotonin, as had been suggested by earlier studies from the Lummis laboratory.[43] This interaction appears to be unique to Trp183. Substitution of the fluorinated Trp series at other aromatic residues in the binding site region causes no significant effects. Interestingly, the slope of the plot relating EC_{50} to calculated cation-π binding energy is rather different than for ACh binding to nAChR. Inspection of Figure 2.9 shows that the serotonin slope is markedly steeper. However, the similarity between these two completely different systems is much more striking than the difference, in light of observations on two highly related agonists at the nAChR.

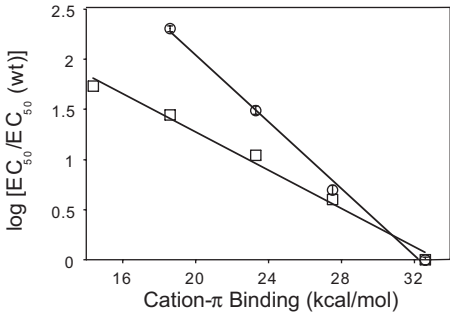

Figure 2.9 Fluorination plots showing dependence of ACh (□) and 5-HT (O) on Trp fluorination at position α149 in βγ L9'S nAChR and 183 in 5-HT_{3A}R. Fluorination plot ($\log[EC_{50}/EC_{50(wt)}]$ versus calculated cation-π binding ability for the series of fluorinated Trp derivatives) for 5-HT data fit the line $y = 5.37 - 0.17x$ and for ACh fit the line $y = 3.2 - 0.096x$. The correlation for both linear fits is $R = 0.99$.

2.3.3 Expected behavior of primary, tertiary, and quaternary ammonium compounds

In comparing ACh, 5-HT, and nicotine, a very evident difference is the nature of the cationic center. ACh contains a quaternary ammonium group, nicotine a tertiary *N*-methyl-pyrrolidinium, and serotonin a primary ammonium. (Figure 2.10) From the standpoint of molecular recognition by aromatic residues, these differences are expected to be significant. The three methyl groups of ACh carry most of the positive charge, and they distribute it relatively diffusely and symmetrically around the nitrogen center. At the opposite extreme, serotonin bears most of the charge of its protonated ammonium on hydrogen atoms close to the nitrogen. The relatively higher charge density of the primary center makes it more attractive to the face of an aromatic amino acid side chain, such as tryptophan. Nicotine occupies a middle ground in terms of cation-π binding ability, but it is important to note as well that the distribution of positive charge around the nitrogen in nicotine is highly asymmetric.

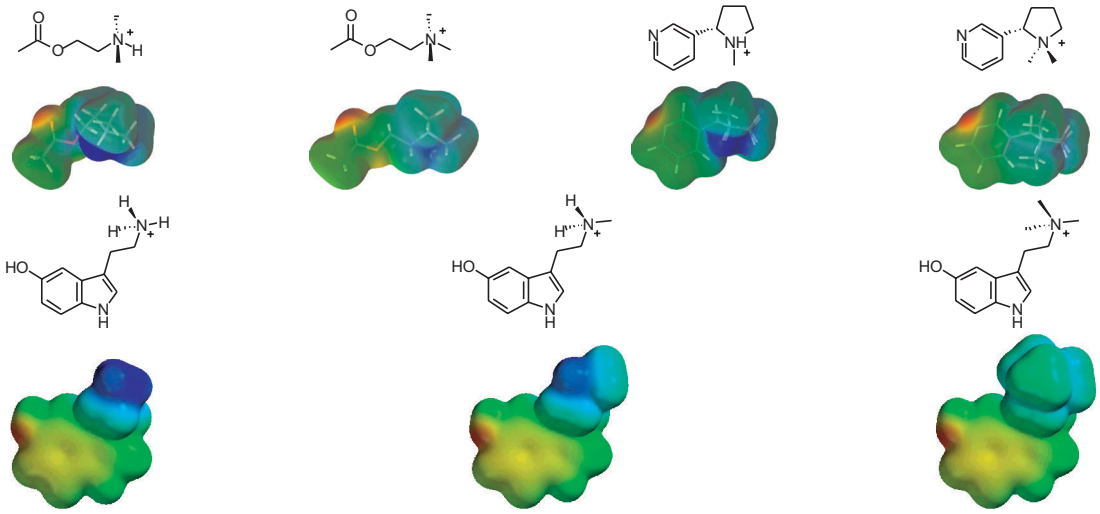

Figure 2.10 Agonists utilized in this study. Top: nAChR agonists with AM1 electrostatic surfaces showing the overall geometrical similarity of the structurally distinct nicotinoid and cholinergic agonists. Bottom: 5-HT_{3A}R agonists, with AM1 electrostatic surfaces showing the varying charge density around the nitrogen center. Electrostatic surfaces were calculated using Spartan and correspond to an energy range of -5 to +160 kcal/mol, where blue is positive and red is negative.

Indeed, all three of these compounds are not modeled at all accurately by considering a spherical distribution of charge, as would be the case for a sodium or potassium atom. As a result, high-level quantum mechanical calculations of the kind performed for fluorinated indoles are not feasible for these cations. The issue of geometry is too important and too difficult to assign to permit any kind of quantitative analysis. However, it is the case that the two molecules which exhibit the hallmark of a cation-π interaction with the Trp homologous to 149 behave as expected from this analysis. In the case of nAChR, the slope of plot of log EC_{50} vs. cation-π binding energy is rather shallow.

Ab initio calculations show that the surface of F_4-Trp is essentially electrostatically neutral.[33,34] Thus, a comparison of F_4-Trp and Trp provides a measure of the *electrostatic component* of the cation-π interaction. The F_4-Trp/Trp ratio reflects the energy cost of removing the attractive electrostatics but maintaining the residue, as if the Trp were

replaced by a hydrophobic residue of the same shape. This new residue maintains most van der Waals and dispersion interactions but cannot experience a cation-interaction. For ACh, the F_4-Trp/Trp ratio is 54. For serotonin, the F_4-Trp EC_{50} value is obtained by extrapolation of the line in Figure 2.9, which leads to a F_4-Trp/Trp ratio of 836. If these are viewed as ratios of binding constants, then the implied energetics of a cation-π interaction are 2.4 and 4.0 kcal/mol, respectively, for ACh and serotonin. These are consistent with other estimates of the magnitude of the cation-π interaction.[10] Based on these calculations, it would appear that the primary cation interacts more strongly with the face of tryptophan.

2.3.4 Experimental behavior of primary and substituted ammonium compounds

Examination of the results for a series of substituted serotonin analogs shows that this simple explanation does not do justice to the complexity of the molecular recognition problem. An *N*-trimethyl version of serotonin has a very similar charge distribution to that seen for ACh. However, Figure 2.11 shows clearly that the slope for this compound is more similar to that of serotonin than that of ACh. Indeed, a secondary analog of serotonin behaves even more like the quaternary version than it does like 5-HT, thus ruling out the hypothesis that slope of this plot reports in a simple way on the strength of the interaction. However, all three of these compounds follow the general trend that we associate with an electrostatic interaction with Trp183. As electron density is withdrawn from the face of the aromatic side chain, the drugs are less and less effective agonists. The EC_{50} rises, in fact, in a fairly regular way with decreasing cation-π binding ability of the aromatic.

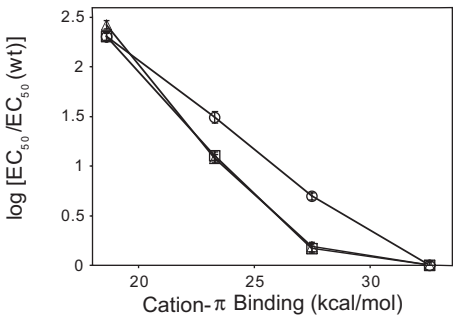

Figure 2.11 Fluorination plots for N-alkylated serotonin analogs showing variation in dependence on Trp fluorination at 5-HT_{3A}R position 183. Agonists are indicated by 5-HT (O), *N*-Me-5-HT ( ), and 5-HTQ (△).

At first glance, these data appear mutually incompatible. On the one hand, EC_{50} can be tuned by varying the attractiveness of the aromatic side chain to the cation. On the other hand, varying the cation-π binding ability of the other partner, the cation, shows no such trend. We interpret this to mean that comparing a series of fluorinated analogs for a given agonist represents the impact of changing electrostatics on a given binding mode, namely, one where the cation is brought within van der Waals contact with the Trp analog. Predictable alteration of the energetics of this interaction gives rise to a predictable trend in EC_{50}. When considering different agonists, however, the comparison is potentially negated by the fact that the binding modes may be different. The distance of the cation from the aromatic face may be different; the geometry may vary, since the highest region of local charge density is probably pointing toward the face of the aromatic; the energetic contribution of other kinds of interactions with other parts of the molecule may differ; and the ability of different agonists to gate the channel may contribute.

2.3.5 Potential acidity of protonated nicotine

Additionally, there is the interesting fact that serotonin analogs differ in a fundamental way from what we have seen with nicotine and ACh. While all the 5-HT analogs show signs of an electrostatic interaction with Trp183, nicotine apparently does not interact in this way with Trp149. Having learned from the 5-HT_3R that cation-π binding ability of the agonist is not a good predictor of dose-response change with increasing fluorination, we considered another hypothesis for nicotine, namely the possibility of deprotonation. Presumably, deprotonation would render the compound unable to bind at all, since no neutral agonists of ligand-gated channels are known. This is a special concern for nicotine, as the pK_a of the pyrrole is decreased to 7.8, almost physiological pH, due to the inductive effect of the pyridyl ring. It is a possibility that the microenvironment of the binding site is such that it buffers the nicotine. This could explain why there is an apparent leveling in the EC_{50} response to increasing fluorination. Rather than reflecting an electrostatic interaction between agonist and receptor, it could be that the assay is reporting on changes in active site basicity as a result of incorporating fluorinated indole side chains. To test this hypothesis, a quaternary derivative of nicotine was analyzed.

2.3.6 Behavior of tertiary and quaternary nAChR agonists

As is readily evident from Figure 2.12, nicotine deprotonation is unable to explain the line shape seen in the plot of log EC_{50} versus cation-π binding ability. *N*-methyl-nicotinium is incapable of being deprotonated, but it gives very similar results to nicotine itself. Certainly, there is no regular increase in EC_{50} with increasing fluorination that characterizes a direct electrostatic interaction with Trp149.

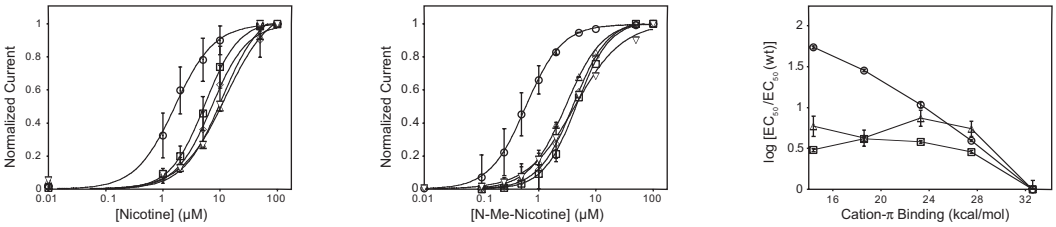

Figure 2.12 Electrophysiological analysis of nicotine and its quaternary analog. Left panel: Nicotine dose-response relations for βγ L9'S nAChR suppressed at α149 with Trp (O), F–Trp (□), F_2-Trp (◊), F_3-Trp (△), and F_4-Trp (▽). Center panel: Dose-response relations for *N*-Me-nicotinium for βγ L9'S receptors suppressed with Trp (O), F–Trp (□), F_2-Trp (◊), F_3-Trp (△), and F_4-Trp (▽) at α149. Right panel: Plot of log [$EC_{50}/EC_{50(wt)}$] for ACh (O), nicotine (□), and *N*-Me-nicotine (△) at the nAChR versus the calculated cation-π binding energy of the series of fluorinated Trp derivatives.

Indeed, nicotine does not experience such an interaction with any of the aromatic amino acids comprising the binding site, as inferred from the AChBP crystal structure. Figure 2.2 shows that substitution of γ55/δ57 with Trp analogs of radically different electrostatic character gives very little difference in EC_{50}. Additionally, earlier studies carried out on Tyr93 and Tyr198 do not show shifts characteristic of nicotine-tyrosine cation-π interactions.[16] Substitution of Tyr190 with even very modestly different unnatural analogs proved impossible, however, so we are unable to rule out the possibility that nicotine interacts with this residue.

Where does this leave us as far as comparing the means of molecular recognition in the two receptors? The expectation for 5-HT_3R was that modulation of the charge density of the cationic center would track with the slope of log EC_{50} versus cation-π binding energy. It stands to reason that the more energetic the interaction between cation and aromatic, the more binding would depend on it. In the simplest case of gas-phase binding of ions to a series of fluorinated Trp's, the slope for Li^+ would be greater than Na^+, which would be greater than K^+, and so on.[10] Clearly, the situation in the binding site is more complicated than this.

Where alkali metal ions are approximately spherical, the charge density of serotonin analogs is highly anisotropic. In fact, shape selection is usually considered to be extremely important in the binding of small molecules in hydrophobic protein active sites.[44] The 5-HT_3R has evolved to bind serotonin, which is a primary amine. Even though 5-HTQ binds and gates with channel with identical potency and efficacy to 5-HT, it is safe to assume that the binding site is optimized for the smaller serotonin cation. The fluoro-Trp-based assay may, in fact, be reporting on extremely subtle differences in positioning, as the electrostatic interaction between cation and π system is strongly distance-dependent. In the case where the natural agonists are being compared, as in 5–HT with 5-HT_3R and ACh with nAChR, it may well be the case that the comparison is significant. Here, the systems are comparable, in that the binding site has been optimized for best fit. The implication that the productive binding mode for 5-HT is more dependent on the electrostatics of Trp183 than is ACh on Trp149 may well be taken to mean that non-cationic interactions with the receptor play a greater role in nAChR.

This interpretation is in some ways consistent with what was observed for TMA by Wenge Zhong.[19] This very simple cation is an agonist of nAChR, but with very low potency. Of all agonists tested, in fact, its potency is the lowest. However, it exhibits a cation-π interaction with Trp149. (Figure 2.13) In other words, productive binding of TMA involves the quaternary ammonium group nestled up against the face of Trp149. From the perspective of the aromatic box, when TMA gets this close, it is quite similar to ACh. The acetyl component of ACh doesn't have room to fit in the box, and probably extends out of the box altogether during productive binding. If TMA looks so similar to ACh at its ammonium head group, then, is it safe to conclude that the additional potency

of ACh comes from interactions between the acetyl group and another part of the binding site? It certainly seems so. This is also in accord with what is observed for nicotine and its *N*-methylated derivative.

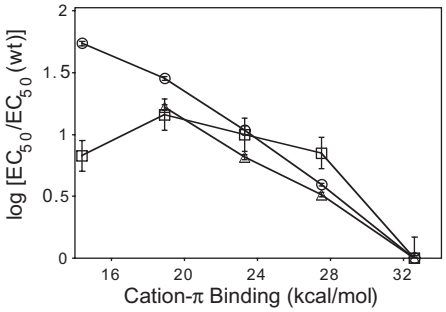

Figure 2.13 Plot of log [$EC_{50}/EC_{50\ (wt)}$] for ACh (O), norACh ( ), and TMA (△) at the nAChR versus the calculated cation-π binding energy of the series of fluorinated Trp derivatives.

Like TMA, these compounds are significantly less potent than ACh. But unlike TMA, they do not appear to come quite so close to the aromatics of the box during their productive binding mode. Indeed, no cation-π interaction is detected with any part of the aromatic box. Nonetheless, the compounds are reasonably efficacious. The conclusion is that the channel can be opened by compounds relying on interactions outside of the aromatic box. The most surprising result of all, *a priori*, is probably the behavior of norACh. (Figure 2.13) The backbone of this compound is identical to ACh. Any non-cationic interaction available to ACh should be equally available to norACh. Indeed, the cationic center of norACh is an even better cation-π binder than the quaternary ammonium of ACh. However, norACh is an agonist of amazingly low potency. It is tempting to conclude that the aromatic box of the nicotinic receptor has evolved to accommodate a quaternary ammonium, and anything smaller is rejected. Until a tertiary compound is discovered which displays an unequivocal cation-π interaction, this argument may even be maintained.

However, it is important to note that nicotine certainly opens the channel without apparently coming in van der Waals contact with the aromatic box. And productive binding is primarily what one is interested in, as far as understanding channel function. The neuronal receptors, for which nicotine is a far more potent agonist than the muscle receptor, will present a very interesting system for study. It is tempting to speculate that these receptors contain aromatic boxes which are more accommodating of nicotine's pyrrolidinium cation and allow it to behave like ACh in all respects. It is also the case that there are hundreds of interesting nicotinic agonists which remain unstudied by this method, including the secondary amine epibatidine. It is highly likely that high-resolution structural data of AChBP may be able to shed further light on the varieties of agonist binding modes.

2.3.7 Conclusions

In conclusion, we have learned several things from these studies. First of all, it is clear that 5-HT experiences a unique cation-π interaction with Trp183. Furthermore, the binding site of 5-HT_3R is such that it can accommodate significant increases in bulk around the ammonium center. Even the quaternary analog retains a direct electrostatic interaction with Trp183 and is an effective agonist for the channel. Second, we have shown that nicotine differs in a dramatic way from ACh in its reliance on direct electrostatic interaction with nAChR Trp149. This finding may prove to be relevant for future generations of nicotinoid drugs. Finally, we have determined that the fluorinated Trp series works well as a general technique. The differences in slope between the EC_{50} vs. cation-π binding energy plots of ACh and serotonin that it reveals may reflect interesting differences in how molecular recognition of neurotransmitters by their

receptors is effected. It remains unwise to generalize too much about the nature of molecular recognition of neurotransmitters by their receptors. The amount of structural information is still too limited. However, elucidation of the atomic-level details of these interactions continues, and the importance of these molecules to biology is so great that we are optimistic that answers will be forthcoming.

2.4 Attempts to introduce unnatural amino acids into neuronal nAChR

2.4.1 Motivation

As indicated above, any serious study of nicotine and its analogs should most properly be carried out on the receptors on which these compounds act. In animals, these receptors are neuronal nAChR.[5,7,8,45] Mice in which either the α4 or β2 nAChR subunits have been genetically knocked out show severely diminished self-administration of nicotine, suggesting that these receptors play a substantive role in the physiological effects of nicotine.[46,47] Additionally, binding studies on brain slices from rats have shown that the majority of nicotine binding in the brain is accounted for by α4β2 and α7 receptors.[48,49]

2.4.2 Expression of α4β2 in oocytes

Literature reports on the expression of α4β2 in oocytes present a variety of EC_{50} values for these receptors.[50-53] Frequently, these differences are attributed to heterogeneity of subunit stoichiometry. This heterogeneity is expected to be a difficult variable to control in a suppression experiment, where the amount of suppressed subunit is difficult to control or predict. In order to assess the behavior of α4β2 receptors in

oocytes, wild-type receptors were expressed prior to the initiation of suppression experiments.

Both α4 and β2 from rat were available in the pAMV subunit, from earlier work in the laboratory by Mark Nowak. In addition to these subunits, mutants containing α L9'S were obtained and expressed. Initially, these receptors gave rather inconsistent results, particularly with regard to dose-response relations. However, it was discovered that changing to pH 6.5 gave much more consistent, and apparently normal behavior. An EC_{50} of 0.99 μM was obtained for ACh from the wild-type receptor, in accord with most published reports.[50-53] (Figure 2.14) The Hill coefficient for this experiment, 0.80, was also in the range of typically reported values.[50-53]

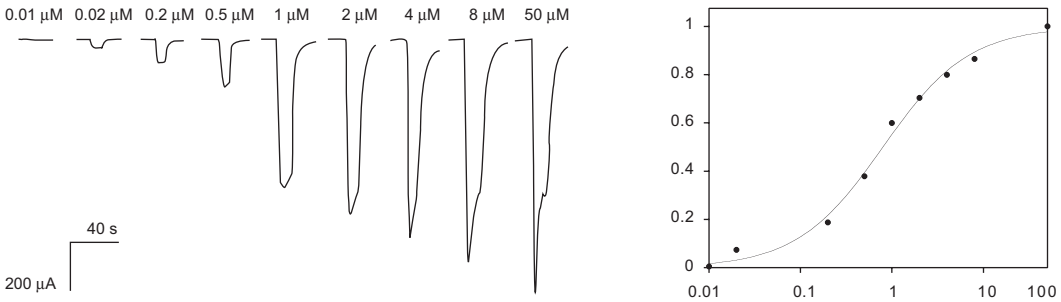

Figure 2.14 ACh dose-response for wild-type rat α4β2 nAChR. Left panel: Individual traces from two-electrode voltage clamp of oocytes treated with the indicated ACh concentrations. Right panel: Dose-response curve for a single oocyte, plotting normalized ACh response against log [ACh] and fitted to the Hill equation.

Because of the presumed stoichiometry of two alpha subunits and three beta subunits, the use of βL9'S subunits was expected to give receptors with a dramatically shifted EC_{50}, so α 9' mutants were used instead. Unfortunately, these receptors proved troublesome to characterize, because of frequent ill effects on oocyte health.

Initial studies attempting to introduce Trp at position α184, homologous to α149 of the muscle receptor, produced absolutely minimal measurable response. Currents were

notably higher for suppression of alpha9' subunits, although these receptors proved difficult to work with, as mentioned above. As the need for optimization became clear, human α4 and β2 subunits were obtained, on the grounds that work on the human receptor would have more direct relevance to the clinical pharmacology of nicotine. Here, the wild-type receptors were obtained from Jon Lindstrom's laboratory in the pSP64 vector. The overall level of expression of both human and rat α4β2 nAChR was noticeably less than that of the mouse muscle receptor, but whole-cell currents of 3-5 μA were routinely obtained.

2.4.3 Initial attempts at wild-type recovery by nonsense suppression

As in the rat receptor, the human α4 W182TAG mutation corresponding to muscle α149TAG was made. Attempts to recover wild-type activity by suppressing with tRNA-Trp were disappointing. The maximum whole-cell currents obtained were on the order of 50 nA, with median values in the range of 20 nA. Co-injection of TAG-containing subunits with wild-type subunits in the absence of suppressor tRNA was performed to test for dominant-negative effects, with no evidence of such an effect. The other residues corresponding the aromatic box of the AChBP were altered to *amber* stop codons and suppressed with Trp. It was observed that the best suppression efficiency was obtained at α182. After many months of optimization, sufficient currents were achieved to collect a dose-response curve for suppressed hα4β2 nAChR. (Figure 2.15) This experiment gave an EC_{50} value of 0.6 ± 0.1 μM, with a Hill coefficient of 1.2 ± 0.1.

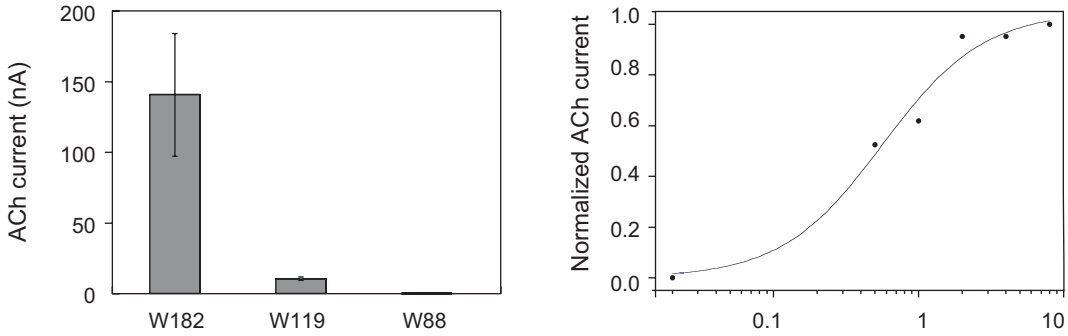

Figure 2.15 Trp suppression of hα4β2 at the indicated position in the alpha subunit. Left panel: Mean whole-cell current (±SEM) in response to 20 μM ACh from oocytes expressing suppressed α4β2 nAChR. Right panel: ACh dose-response curve from a single oocyte suppressed with Trp at position hα4-182. In all cases, 30 ng total mRNA (50:1 hα4-W182TAG:β2) was injected, and recordings made 48 hr post-injection in ND96, pH 6.5.

However, such expression levels were not typical, and even these whole-cell currents were barely adequate for obtaining dose-response relations. It appeared that poor suppression efficiency was characteristic of α4β2 nAChR. Accordingly, a broad-based program to boost expression was undertaken.

2.4.4 Increasing translational efficiency

2.4.4.1 Use of vectors optimized for oocyte expression

One possible reason for low expression is that the suppressed subunits are not being efficiently translated. Given the importance of heterologous expression in *Xenopus* oocytes to ion channel biology, a number of expression vectors have been developed and optimized for expression in this system. A vector developed in the Lester laboratory, pAMV, has typically given good results. This vector contains a 3' UTR from alfalfa mosaic virus, which is thought to confer upon the mRNA the ability to bind relatively well to free ribosomes, thus providing a competitive advantage over endogenous mRNA.[54,55] Another common strategy for vector design has been to flank the desired gene with 5' and 3' UTR from a highly expressed gene, such as β-globin.[56] A vector

containing a multiple-cloning site surrounded by *Xenopus* β-globin UTR was obtained, along with several others which have been reported to produce high levels of expression in oocytes.

Unfortunately, two of these vectors (pBSTAII and pNKS)[56,57] proved difficult to clone the hα4 and hβ2 subunits into, and another gave no expression at all (pSGEM).[58] The complete lack of expression with pSGEM gave reason to believe that the latter constructs were faulty, although restriction digestion and sequencing of the gene region appeared normal. Some favorable results were obtained with pAMV, particularly where expression was measured two days after injection. (Figure 2.16)

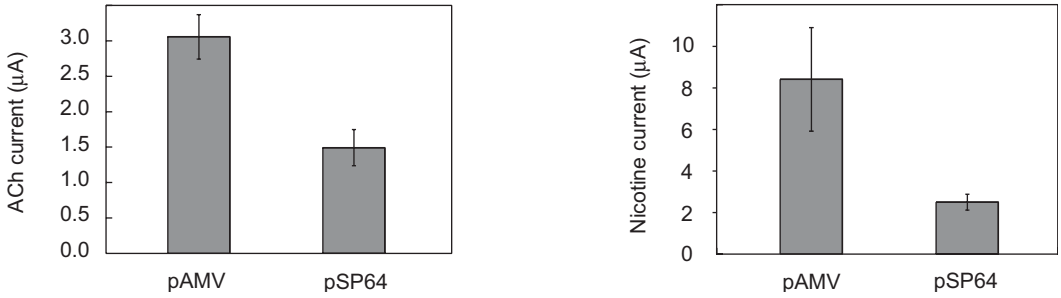

Figure 2.16 Comparison of pAMV and pSP64 vectors for wild-type hα4β2 expression. Left panel: Mean whole-cell currents (±SEM) in response to 20 μM ACh. Right panel: Mean whole-cell currents (±SEM) in response to 20 mM nicotine. In all cases, 27.5 ng total mRNA (10:1 α4:β2) were injected. Recordings were made 48 hr subsequent to injection, at pH 6.5.

Whether or not this advantage is germane to suppression experiments remains to be tested.

2.4.4.2 Overexpression of elongation factors

Another strategy which may increase translation is to boost the level of proteins associated with translation. One translation factor which is considered a promising candidate for such up regulation is EF-1α.[59] This elongation factor binds to aminoacylated tRNA. There is some evidence suggesting that this binding stabilizes the

charged tRNA toward hydrolysis, which would be desirable.[60] In addition, it is the ternary complex of EF-1α, GTP, and aminoacyl tRNA which binds to the A site of the ribosome in translation.[61,62] The oocyte isoform of *Xenopus* EF-1α has been cloned, but repeated requests for these constructs were ignored.[63,64] Adult *Xenopus* EF-1α was available, as the control RNA in the Ambion mMagic mMessage kit routinely used in the laboratory to produce mRNA *in vitro*, and was also obtained from Paul Krieg.[65] The two isoforms are quite similar, so experiments were carried out with the adult isoform.

In a typical experiment, mRNA coding for EF-1α was injected 24 hours prior to the injection of oocytes with nAChR mRNA. Co-injection was also attempted, as well as injection at a variety of intervals prior to nAChR mRNA injection. Both wild-type and suppressed receptors were examined. In no case was a significant difference observed relative to control oocytes.

2.4.5 Promoting folding, assembly, and transport to the plasma membrane

2.4.5.1 Use of epitope tags as a diagnostic

In addition to possible translational inefficiency, it may be that poor expression results from compromised folding of suppressed subunits, assembly of subunits into functional receptors, or transport of receptors to the plasma membrane. Whether folding and assembly or trafficking is the primary problem may be addressed by biochemical analysis. Synthesis of receptor subunits may be detected through Western blotting, a technique which is treated in much greater depth in Chapter 3. In brief, a crude protein isolate from oocytes expressing the desired receptor is prepared and subject to gel electrophoresis. The proteins are thus separated by size. They may be transferred to

nitrocellulose, which is probed by antibodies. The use of antibodies which specifically recognize an antigenic determinant introduced in an epitope tag results in specific labeling of the protein containing the epitope tag. This technique is of value here, because membrane preparations from the plasma membrane of the cell may be compared to those from the cytoplasm. If receptors are being synthesized but improperly trafficked, this will be evident from staining of cellular membranes but not those from the plasma membrane.

The HA epitope tag was introduced into the hα4 subunit, in two places, a region in the M3-M4 loop previously determined not to affect expression of the muscle-type receptor, and at the extreme C-terminus of the subunit. Whole-cell currents from these two constructs were compared to those of oocytes expressing wild-type α4β2. While current was almost completely eliminated in the C-terminal receptor, only a modest diminution was observed for the M3-M4 HA tag. These results were corroborated by Western blots, both with protein produced *in vitro* and from the plasma membrane of oocytes expressing the two different constructs.

Whether or not the HA tag will prove to be a useful diagnostic in following trafficking of suppressed receptors awaits introduction of the epitope tag into TAG-containing subunits.

2.4.5.2 Co-expression of dominant-negative dynamin

The presence of receptors on the cell surface is the result of a dynamic equilibrium between forward trafficking from the ER and removal from the membrane by endocytosis. A dominant-negative dynamin mutant is available which greatly reduces clathrin-mediated endocytosis.[66,67] In certain cases, disruption of dynamin activity in

Xenopus oocytes has been reported to increase ion channel expression severalfold.[68,69] In experiments with α4β2, no increase was observed through co-injection with dominant-negative dynamin, nor was suppression efficiency improved.

2.4.5.3 Overproduction of BiP

The folding of membrane proteins is thought to be assisted by a number of ER-resident chaperones. Probably the best-characterized is BiP, a soluble protein present in the ER lumen. This protein has been expressed in *Xenopus* oocytes by the laboratory of Käthi Geering.[70] The construct was obtained from her laboratory, and experiments similar to those reported above for EF-1α were carried out. As with the elongation factor experiments, co-expression of wild-type and W182-suppressed hα4β2 nAChR with BiP appeared to have little effect.

2.4.5.4 FAYENE insertion

A study on expressing potassium channels in oocytes has suggested that the sequence FCYENE is a forward-trafficking signal for these channels, which increased expression four- to fivefold in heterologous expression in *Xenopus* oocytes.[71] The report also suggested that transferring this sequence to other channels had a similar effect, and that the sequence FAYENE was likewise effective. In order to avoid any complications associated with introducing a cysteine residue, the sequence FAYENE was introduced into hα4 in the same M3-M4 position which had proven successful for the introduction of the HA epitope. Comparison of these modified receptors with wild-type hα4 revealed no apparent benefit of this sequence on whole-cell expression levels.

2.4.6 Alternative strategies for increasing expression

2.4.6.1 Chimeric receptors

An altogether different strategy for circumventing the expression problems of α4β2 is the use of chimeric subunits. The increased expression of 5-HT_3R relative to α7 nAChR has been traced to its transmembrane regions.[72] The discovery by Changeux that a chimera between the extracellular domain of α7 and the TM domains of 5-HT_{3A}R shows the binding properties of the α7 AChR raises the possibility that binding-site studies could be carried out on chimeric receptors.[29] The α4/5-HT_3 and β2/5-HT_3 chimeras have been generated in the laboratory of Neil Millar and have been reported to assemble, although no functional studies have yet been carried out.[31,32] Nonetheless, these constructs were obtained and injected. A 1:1 mRNA ratio was initially employed, as the stoichiometry of this chimera between a heteromeric and homomeric receptors is difficult to predict. This initial experiment gave no observable whole-cell ACh current, nor did any variation of the relative amounts of mRNA improve upon this result. It may be the case that these chimeras are simply non-functional. No binding studies were undertaken, as the ultimate purpose of the experiment was to obtain functional data.

2.4.6.2 Multiple injection

A conceptually simple and usually effective method for increasing expression in *in vivo* nonsense suppression is to multiply inject oocytes, typically at 24-hour intervals. It was this technique coupled with the use of the pAMV vector which gave the best suppression results to date in α4β2 nAChR. (Figure 2.17)

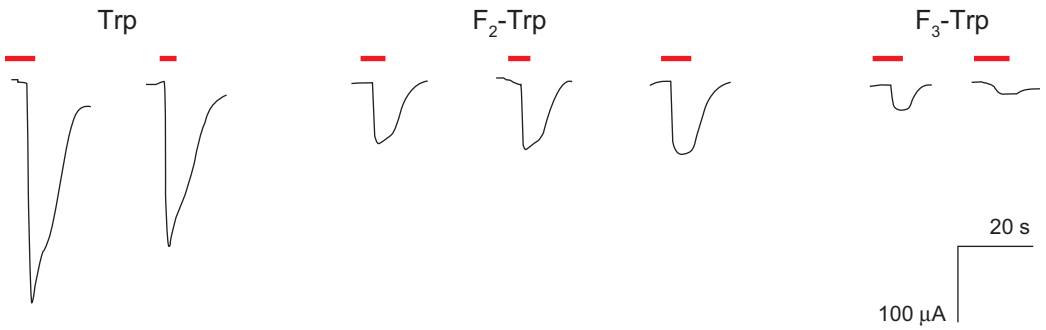

Figure 2.17 Individual traces from two-electrode voltage clamp of oocytes expressing hα4β2 suppressed with the indicated residue at position 182 of the α4 subunit. Oocytes were double-injected (t = 0, and t = 24 hr) with 25 ng total mRNA (1:1 α4:β2) and recorded from 48 hrs after the initial injection. Currents are in response to 50 μM ACh, and red bars indicate the duration of its application.

These whole-cell currents are of sufficient magnitude that dose-response curves could be measured. Disappointingly, however, currents this large were unable to be obtained for any fluorinated Trp residue, precluding the desired characterization of cation-π interactions in neuronal nAChR.

2.4.7 Conventional mutagenesis experiments

A final experiment was undertaken to attempt to shed light on the differing modes of nicotine and ACh binding between muscle and neuronal receptors. The affinity of the muscle-type receptor for ACh is significantly greater than its affinity for nicotine, as noted above. For all neuronal receptors tested, this affinity is reversed.[50-53] In addition, the muscle alpha subunit is alone among all discovered nAChR subunits in having an arginine residue at the 55 position. Every other subunit contains a tryptophan at this position. Even though our results above do not indicate a special relationship between γ55/δ57 and nicotine in the muscle receptor, the photoaffinity experiments of Cohen are suggestive of such a relationship.[20] As a result, this residue was targeted for alteration by

site-directed mutagenesis, and the relative potency of ACh and nicotine were tested on the resulting mutants.

In the muscle receptor, an αR55W mutation was made and in hα4, W88R. The whole-cell currents in response to a variety of ACh and nicotine concentrations were measured, in hopes of observing an alteration of the usual pattern of ACh and nicotine potency. (Figure 2.18) The potency difference between ACh and nicotine at the muscle receptor may be seen from the behavior of the wild-type receptor in response to three concentrations of each agonist, 1 μM, 10 μM, and 100 μM. The αR55W mutant seems to have diminished ACh affinity, but without a corresponding increase in that of nicotine.

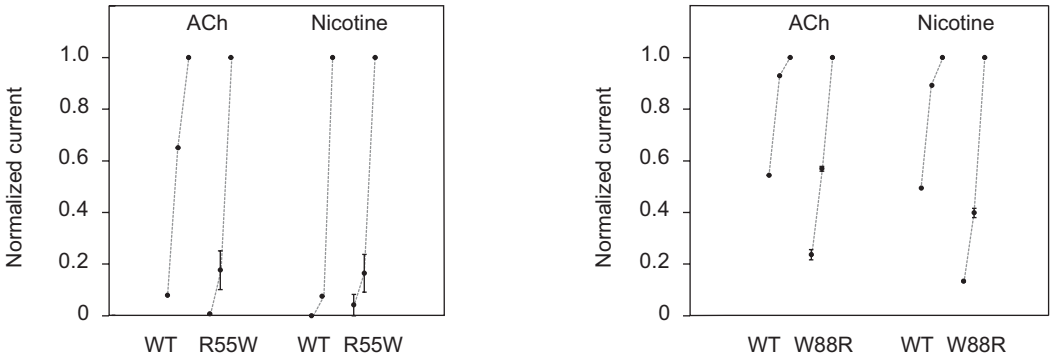

Figure 2.18 Conventional mutagenesis of the position homologous to α55 in muscle nAChR in muscle (R55W) and hα4β2 (W88R). Whole-cell currents in response to 1, 10, and 100 μM ACh and nicotine, as indicated, are shown after normalization to the response to 100 μM agonist. In cases where multiple experiments were performed, SEM is indicated. Dotted line is a guide only, not a fitting of the data. Left panel: Comparison of wild-type and αR55W muscle nAChR response to ACh and nicotine. Right panel: Responses of wild-type and W88R hα4β2 to ACh and nicotine.

The responses of wild-type hα4β2 to both ACh and nicotine were almost identical. Likewise, the response of the mutant W88R receptors to both agonists is very similar. For both, the apparent effectiveness has been decreased in the mutant receptor, but without the predicted switch in potency. It is possible that detailed dose-response studies of these mutants may reveal some interesting trends. This initial study utilized only three

concentrations of agonist, and concentrations that lie in very different regions of the dose-response curve for ACh and nicotine, both of which may mask small effects on potency. However, no dramatic reversal of ACh and nicotine affinities was observed, suggesting that the identity of this residue is not determinative of relative affinity for ACh and nicotine.

2.4.8 Future directions

In order to precisely establish the role of cation-π interactions in agonist binding to neuronal receptors, it is necessary to develop relatively robust methodology for introducing unnatural amino acids. Thus far, the usual methodology applied successfully to so many other receptors in this laboratory has failed to yield sufficiently large whole-cell currents to obtain the necessary dose-response relations for α4β2 nAChR. Through the use of the pAMV vector and multiple injections, useful currents can relatively reproducibly be obtained for suppression of α182 with Trp. Attempts to extend to fluorinated Trp derivative have thus far been unsuccessful. A number of directions could be pursued to perhaps achieve this goal.

First, recent results from the work of Nivalda Rodrigues-Pinguet and Bruce Cohen in the Lester laboratory suggest that a threefold increase in whole-cell current from α4β2-expressing oocytes may be achieved by potentiation with 3 mM Ca^{2+}. Although careful controls would be required to verify that this potentiation is not accompanied by any alteration in agonist affinity, this may be a simple and useful means to obtain usable currents via nonsense suppression. Second, there is reason to believe that the four-base suppression methodology of Sisido *et al*. may give greater suppression efficiency than *amber* suppression.[73] Indeed, generation of the requisite constructs and tRNA's with

four-base anticodons was planned and undertaken, but difficulties in preparing them prevented this methodology from being tested. Third, there is the possibility that alpha7 nAChR, also thought to be an important pharmacological target for nicotine, may be more amenable to nonsense suppression in oocytes. Hong Dang, in the Lester laboratory, has made the TAG mutant homologous to Trp149 in the chimeric construct rα7V201/r5-HT_3-AMV. However, somewhat contrary to expectation, this construct expressed very poorly in his hands. In addition, we have the 'WT' version of this construct as well as rα7 and cα7, both in the pAMV vector. Because of our success with suppression in homomeric 5-HT_3, there is perhaps reason to be optimistic that suppression will work equally well in α7. In addition, there is an interesting observation in the literature that cocaine (a tertiary amine) is not an agonist of α7, while the quaternary cocaine methiodide is a rather good agonist.[74]

In general, identification of the molecular details which account for the difference in potency between nicotine and ACh for muscle and neuronal nAChR is an interesting question. The conclusions from the fluorinated Trp study on the muscle receptor could be augmented by studies on neuronal receptors that do not rely on nonsense suppression. For instance, despite the similarity noted above in the muscle-type receptor's response to nicotine and the perpetually charged *N*-methyl-nicotinium analog, it may be the case that neuronal receptors respond differently to these agonists. In addition to pharmacological studies of this nature, there is the possibility that comparison of the sequence similarities and differences among AChBP, muscle receptors, and neuronal nAChR may provide a guide for future experimentation.

2.5 Experimental methods

2.5.1 Electrophysiology

Stage VI oocytes of *Xenopus laevis* were harvested according to procedures approved by the Institute. Recordings were made 24-72 hours post-injection in standard two-electrode voltage clamp mode. Oocytes were perfused in calcium-free ND96 solution, as previously reported.[1] Nicotinic agonists were either synthesized as described earlier (N-methyl-nicotinium),[22] purchased from Sigma/Adrich/RBI ([-]-nicotine tartrate) or Acros Organics (the tertiary ACh analog, 2-dimethyl aminoethyl acetate). Serotonin and its analogs were purchased from Sigma/Adrich/RBI. All drugs were prepared in sterile ddi water for dilution into calcium-free ND96. Dose-response data were obtained for a minimum of eight concentrations of agonists for a minimum of three different cells. Curves were fit to the Hill equation to determine EC_{50} and Hill coefficient.

2.5.2 Unnatural amino acid suppression in muscle nAChR and 5-HT_{3A}R

Synthetic amino acids were conjugated to the dinucleotide dCA and ligated to truncated 74 nt tRNA as described.[75] Deprotection of charged tRNA was carried out by photolysis immediately prior to co-injection with mRNA, in the manner described.[1,76] Typically, 25 ng tRNA were injected per oocyte along with mRNA in a total volume of 50 nL per cell. mRNA was prepared by *in vitro* runoff transcription using the Ambion mMagic mMessage kit. Mutation to insert the *amber* stop codon at the site of interest was carried out by standard means and was verified by sequencing through both strands. For nAChR suppression, a total of 4.0 ng of mRNA was injected in the subunit ratio of 10:1:1:1 α:β:γ:δ. In many cases, non-α subunits contained a L9'S mutation, as discussed

below. Mouse muscle embryonic nAChR in the pAMV vector was used, as reported previously. For suppression in homomeric 5-HT_3R, 5 ng of mRNA were injected. Experiments involving heteromeric 5-HT_{3A} and 5-HT_{3B} subunits employed a total of 4.0 ng of mRNA in the subunit ratio of 10:1A:B.[77] Mouse 5–HT_{3A}R was used in all cases, in the pAMV vector. Negative and positive controls for suppression were performed in the following way. As a negative control, truncated 74 nt tRNA or truncated tRNA ligated to dCA were co-injected with mRNA in the same manner as fully charged tRNA. At the positions studied here, no current was ever observed from these negative controls. The positive control involved wild-type recovery by co-injection with 74 nt tRNA ligated to dCA-Trp. In all cases, the dose-response was indistinguishable from injection of wild-type mRNA alone.

2.5.3 Molecular biology of α4β2

In the course of attempting to introduce unnatural amino acids into α4β2 nAChR, numerous constructs were made and obtained. They are listed in Table 2.6. All pSP constructs were linearized with *AseI* and then transcribed using the mMagic mMessage SP6 kit. pAMV constructs relied upon *NotI*/T7, in the usual fashion. The pSGEM constructs we made gave no expression at all. Additionally, testing the integrity of individual subunits by co-injection with partners of known integrity (pSGEM-α4 + pAMV-β2 and pAMV-α4 + pSGEM-β2) failed to result in expression. Sequencing of the region of sub-cloning appeared normal. The *SfiI*-linearized pSGEM DNA gave the appropriate UV spectrum. The mRNA produced by the T7 kit was analyzed by agarose gel electrophoresis and appeared very similar in size to α4 and β2 transcribed from pSP

and pAMV constructs. Nonetheless, it is likely that these constructs were faulty in some way. In all of the above experiments, mRNA amounts were not well controlled. The quantities injected were estimated by comparing mRNA band intensity on agarose gels to that of pSP-α4 and pSP-β2 mRNA, and then diluting to give similar band intensities, but this is a rather rough measure.

Construct	Comments	Source
pSP64-hα4		Jon Lindstrom
pSP64-hα5		Jon Lindstrom
pSP64-hβ2		Jon Lindstrom
pAMV-hα4		GSB/LJT
pAMV-hβ2		GSB/LJT
pSP64-hα4/M3-M4HA	contains HA epitope	GSB/LJT
pSP64-hα4/CTHA	contains HA epitope	GSB/LJT
pSP64-hα4/W88TAG	Trp55 homolog	GSB/LJT
pSP64-hα4/W119TAG	Trp86 homolog	GSB/LJT
pSP64-hα4/W182TAG	Trp149 homolog	GSB/LJT
pSGEM-hα4	failed to express	GSB/LJT
pSGEM-hβ2	failed to express	GSB/LJT
BiP		Käthi Geering
EF-1α		Paul Krieg
pSGEM		Andreas Karschin
pBSTAII	difficult to clone into	Ligia Toro
pNKS	difficult to clone into	Gunther Schmalzing
pRK5-rα4/m5-HT_3		Neil Millar
pRK5-rβ2/m5-HT_3		Neil Millar

Table 2.6 List of constructs utilized in α4β2 suppression studies.

The BiP construct was linearized with *BglII* and transcribed using the SP6 kit.[70] With regard to *Xenopus* oocyte EF-1α, Jane Frydenberg never responded to our e-mail request for this clone. Andre Mazabraud and Herman Denis at CNRS, Gif-Sur-Yvette also failed to reply. In the end, Paul Krieg at the University of Texas, sent us a plasmid containing the adult form of *Xenopus* EF-1α.[65] The experiments performed with EF-1α, however, utilized adult Xef1, which is included as a control plasmid in Ambion kits, because of its robustness in *in vitro* translation. The linearized plasmid is included, and was transcribed using the T7 kit. Neil Millar's α4/5-HT_3 and β2/5-HT_3 constructs were linearized with *KpnI* and transcribed using the SP6 kit.[31,32]

Suppression in hα4 was attempted with Trp at positions 88, 119, and 182 (homologous to 55, 86, and 149 in muscle), despite the fact that the TAG mutants were all in the pSP construct. Low, but perhaps usable expression was observed at 182. In some experiments, mean currents of about 250 nA were observed, with individual oocytes giving as much as 500 nA. The very mRNA mixes used in these experiments had consistently given only 20 nA currents over a year previously. It may be that this increase in suppression resulted from improvements that James Petersson made during this time in the arc lamp setup. None of these experiments was rigorously controlled with 74mer, although whenever we did suppress with 74mer, we got no current at all. In addition, a methodical study of subunit amounts and ratios was not carried out.

Since reasonable currents were being obtained with the hα4β2 mRNA mixes, an attempt was made to introduce the 5-CN- and 5-Br-Trp pair at position 182. Both times it was tried, no currents were observed. However, it was also the case that Trp suppression on both days was giving much less than 50 nA whole-cell current. The second time, all three amino acids (Trp, CN-W, and Br-W) were double-injected, but these oocytes failed to express even WT nAChR. In general, there were oocyte problems throughout the laboratory concurrent with these experiments.

Nicotine experiments were performed at pH 6.5, as were most ACh experiments. In general, ACh in pH 6.5 Ca^{2+}-free ND96 gave the same current as it did at pH 7.5, which is the normal pH of recording solution.

2.5.4 Introduction of the HA epitope into hα4

The HA epitope was successfully introduced into pSP-α4, at a position in the M3-M4 loop *[PPQQPLEAE*KASPHP]* homologous to the traditional 347 position (see Chapter

3) in muscle alpha, and also at the C-terminus immediately before the TAA codon *[WLAGMI*]*. By *in vitro* translation, both constructs gave intense staining at about 55 kDa in a Western blot with BAbCo anti-HA antibody, using the usual protocol. Electrophysiologically, we saw absolutely no current with the C-terminal tag construct and about 78% of WT current with the M3-M4 HA construct. mRNA levels were reasonably consistent among the three constructs, but it would be unwise to rely too much on these experiments for quantitative current comparisons, which were not our intent in this study. Membranes manually dissected from the very oocytes used for the electrophysiology showed absolutely no staining for the WT and C-terminal constructs and very clear, intense staining at unusually large molecular weights (doublets at ~100 kDa and ~200 kDa) for the M3 construct. However, all of these experiments were done only once each.

During the course of various experiments, we saw small but measurable currents from an alpha subunit co-injected with non-coding mRNA (in one case, for instance, the mRNA was run off from a β2 construct where we had ordered a faulty primer and inserted a frameshift in the second amino acid). This may be something to be careful of in future experiments.

2.5.5 Planning for four-base codon suppression

The most successful reported four-base suppression in both *E. coli* and rabbit reticulocyte extracts employed the codon *CGGG*.[78] In addition, *AGGT* was reported to work well in *E. coli* extracts.[73] In *Xenopus laevis*, *AGG* is fairly common (12.3 occurrences per thousand), whereas *CGG* is rather uncommonly used (6.0 per thousand).[79] In *E. coli*, these numbers are 1.7 for *AGG* and 5.4 for *CGG*. Least common non-stop codons in *Xenopus* are *UCG* (3.9), *ACG* (4.6), *GCG*

(4.7), and *CCG* (4.8). Comparable numbers for *E. coli* are *UCG* (8.6), *ACG* (13.8), *GCG* (31.8), and *CCG* (22.0).[79] As a result, we chose to emulate the strategy of Sisido in employing *AGGT*, but also in order to minimize competition with endogenous tRNA's, we also chose a codon based on the least-used coding triplet, *UCG*. The fourth base was somewhat arbitrarily made a *G*, giving *TCGG*. The initial experiments were specifically intended to increase the suppression efficiency of hα4-W182 relative to conventional *amber* suppression with TH73G-Trp. Thus, we planned to prepare two mRNA's, namely hα4 W182 *CGGG* and hα4 W182 *TCGG*.

We also chose to utilize two different kinds of tRNA. One followed the strategy of Sisido, and the other was derived from what is known to work for suppression in *Xenopus* oocytes.[73,78,80,81] Sisido's suppressor tRNA is based on yeast Phe, quite similar to our MN3. We planned to use a version where nucleotide 73 has been changed to A, referred to as YF73G. In addition, we designed a modified TH73G to recognize the above four-base codons. In total, we planned to prepare five tRNA's, YF73G *CCCG*, TH73G *CCCG*, YF73G *CCGA*, TH73G *CCGA*, and YF73G *CUA*. Difficulties in preparing the above constructs prevented us from trying four-base suppression, although it may be an interesting strategy for future attempts to suppress in α4β2 nAChR.

2.6 References

1. Zhong, W. G. et al. From ab initio quantum mechanics to molecular neurobiology: A cation-pi binding site in the nicotinic receptor. *PNAS* **95**, 12088-12093 (1998).
2. Mishina, M. et al. Expression of functional acetylcholine-receptor from cloned cDNA. *Nature* **307**, 604-608 (1984).
3. Arias, H. R. Topology of ligand binding sites on the nicotinic acetylcholine receptor. *Brain Res. Rev.* **25**, 133-191 (1997).
4. Arias, H. R. Binding sites for exogenous and endogenous non-competitive inhibitors of the nicotinic acetylcholine receptor. *Biochim. Biophys. Acta* **1376**, 173-220 (1998).
5. Corringer, P. J., Le Novere, N. and Changeux, J. P. Nicotinic receptors at the amino acid level. *Ann. Rev. Pharm.* **40**, 431-458 (2000).
6. Hucho, F. and Weise, C. Ligand-gated ion channels. *Angew. Chem. Int. Ed. Eng.* **40**, 3100-3116 (2001).
7. Jones, S., Sudweeks, S. and Yakel, J. L. Nicotinic receptors in the brain: correlating physiology with function. *Trends Neurosci.* **22**, 555-561 (1999).

8. McGehee, D. S. and Role, L. W. Physiological diversity of nicotinic acetylcholine receptors expressed by vertebrate neurons. *Ann. Rev. Physiol.* **57**, 521-546 (1995).
9. Miyazawa, A., Fujiyoshi, Y., Stowell, M. and Unwin, N. Nicotinic acetylcholine receptor at 4.6 Å resolution: transverse tunnels in the channel wall. *J. Mol. Biol.* **288**, 765-786 (1999).
10. Ma, J. C. and Dougherty, D. A. The cation-pi interaction. *Chem. Rev.* **97**, 1303-1324 (1997).
11. Dougherty, D. A. and Stauffer, D. A. Acetylcholine binding by a synthetic receptor - implications for biological recognition. *Science* **250**, 1558-1560 (1990).
12. Brejc, K. et al. Crystal structure of an ACh-binding protein reveals the ligand-binding domain of nicotinic receptors. *Nature* **411**, 269-276 (2001).
13. Galzi, J. L. et al. Mutations in the channel domain of a neuronal nicotinic receptor convert ion selectivity from cationic to anionic. *Nature* **359**, 500-505 (1992).
14. Labarca, C. et al. Channel gating governed symmetrically by conserved leucine residues in the M2 domain of nicotinic receptors. *Nature* **376**, 514-516 (1995).
15. Kearney, P. C. et al. Interactions of leucine residues at the 9' position of the M2 domain of the AChR probed using unnatural amino acid mutagenesis. *Biophys. J.* **70**, Tuam5-Tuam5 (1996).
16. Kearney, P. C., Zhang, H. Y., Zhong, W., Dougherty, D. A. and Lester, H. A. Determinants of nicotinic receptor gating in natural and unnatural side chain structures at the M2 9' position. *Neuron* **17**, 1221-1229 (1996).
17. Jackson, M. B. and Yakel, J. L. The 5-HT_3 receptor channel. *Ann. Rev. Physiol.* **57**, 447-468 (1995).
18. Kearney, P. C. et al. Dose-response relations for unnatural amino acids at the agonist binding site of the nicotinic acetylcholine receptor: tests with novel side chains and with several agonists. *Mol. Pharm.* **50**, 1401-1412 (1996).
19. Zhong, W. *Ph.D. Thesis* (California Institute of Technology, Pasadena, CA, 1998).
20. Xie, Y. and Cohen, J. B. Contributions of *Torpedo* nicotinic acetylcholine receptor gamma Trp-55 and delta Trp-57 to agonist and competitive antagonist function. *J. Biol. Chem.* **276**, 2417-2426 (2001).
21. Chiara, D. C., Middleton, R. E. and Cohen, J. B. Identification of tryptophan 55 as the primary site of [3H]nicotine photoincorporation in the gamma-subunit of the *Torpedo* nicotinic acetylcholine receptor. *FEBS Lett.* **423**, 223-226 (1998).
22. Seeman, J. I. and Whidby, J. F. The iodomethylation of nicotine. An unusual example of competitive nitrogen alkylation. *J. Org. Chem.* **41**, 3824-3826 (1976).
23. Cho, A. K., Jenden, D. J. and Lamb, S. I. Rates of alkaline hydrolysis and muscarinic activity of some aminoacetates and their quaternary ammonium analogs. *J. Med. Chem.* **15**, 391-399 (1972).
24. Petersson, E.J. *Biochemisry*, in press. (2002).
25. Kenakin, T. Efficacy in drug receptor theory: outdated concept or under-valued tool? *Trends Pharm. Sci.* **20**, 400-405 (1999).
26. Kenakin, T. Inverse, protean, and ligand-selective agonism: matters of receptor conformation. *FASEB J.* **15**, 598-611 (2001).
27. Colquhoun, D. Binding, gating, affinity and efficacy: the interpretation of structure-activity relationships for agonists and of the effects of mutating receptors. *Br. J. Pharm.* **125**, 924-947 (1998).
28. Dineley, K. T. and Patrick, J. W. Amino acid determinants of alpha 7 nicotinic acetylcholine receptor surface expression. *J. Biol. Chem.* **275**, 13974-13985 (2000).
29. Eisele, J. L. et al. Chimeric nicotinic serotonergic receptor combines distinct ligand-binding and channel specificities. *Nature* **366**, 479-483 (1993).
30. Rakhilin, S. et al. alpha-Bungarotoxin receptors contain alpha 7 subunits in two different disulfide-bonded conformations. *J. Cell Biol.* **146**, 203-217 (1999).
31. Harkness, P. C. and Millar, N. S. Inefficient cell-surface expression of hybrid complexes formed by the co-assembly of neuronal nicotinic acetylcholine receptor and serotonin receptor subunits. *Neuropharmacology* **41**, 79-87 (2001).
32. Cooper, S. T., Harkness, P. C., Baker, E. R. and Millar, N. S. Up-regulation of cell-surface alpha 4 beta 2 neuronal nicotinic receptors by lower temperature and expression of chimeric subunits. *J. Biol. Chem.* **274**, 27145-27152 (1999).
33. Mecozzi, S., West, A. P. and Dougherty, D. A. Cation-pi interactions in simple aromatics: Electrostatics provide a predictive tool. *J. Am. Chem. Soc.* **118**, 2307-2308 (1996).

34. Mecozzi, S., West, A. P. and Dougherty, D. A. Cation-pi interactions in aromatics of biological and medicinal interest: Electrostatic potential surfaces as a useful qualitative guide. *PNAS* **93**, 10566-10571 (1996).
35. Maricq, A. V., Peterson, A. S., Brake, A. J., Myers, R. M. and Julius, D. Primary structure and functional expression of the $5HT_3$ receptor, a serotonin-gated ion channel. *Science* **254**, 432-437 (1991).
36. Boess, F. G. et al. Analysis of the ligand binding site of the $5\text{-}HT_3$ receptor using site directed mutagenesis: importance of glutamate 106. *Neuropharmacology* **36**, 637-647 (1997).
37. Curtis, L. et al. A new look at the neuronal nicotinic acetylcholine receptor pharmacophore. *Eur. J. Pharm.* **393**, 155-163 (2000).
38. Schmitt, J. D. Exploring the nature of molecular recognition in nicotinic acetylcholine receptors. *Curr. Med. Chem.* **7**, 749-800 (2000).
39. Schmitt, J. D., Sharples, C. G. and Caldwell, W. S. Molecular recognition in nicotinic acetylcholine receptors: the importance of pi-cation interactions. *J. Med. Chem.* **42**, 3066-3074 (1999).
40. Sheridan, R. P., Nilakantan, R., Dixon, J. S. and Venkataraghavan, R. The ensemble approach to distance geometry: application to the nicotinic pharmacophore. *J. Med. Chem.* **29**, 899-906 (1986).
41. Tonder, J. E. et al. Improving the nicotinic pharmacophore with a series of (isoxazole)methylene-1-azacyclic compounds: synthesis, structure-activity relationship, and molecular modeling. *J. Med. Chem.* **42**, 4970-80 (1999).
42. Tonder, J. E. and Olesen, P. H. Agonists at the alpha4beta2 nicotinic acetylcholine receptors: structure-activity relationships and molecular modelling. *Curr Med Chem* **8**, 651-674 (2001).
43. Spier, A. D. and Lummis, S. C. The role of tryptophan residues in the 5-Hydroxytryptamine(3) receptor ligand binding domain. *J. Biol. Chem.* **275**, 5620-5625 (2000).
44. Davis, A. M. and Teague, S. J. Hydrogen bonding, hydrophobic interactions, and failure of the rigid receptor hypothesis. *Angew. Chem. Int. Ed. Eng.* **38**, 737-749 (1999).
45. Lena, C. and Changeux, J. P. Pathological mutations of nicotinic receptors and nicotine-based therapies for brain disorders. *Curr. Op. Neurobiol.* **7**, 674-682 (1997).
46. Picciotto, M. R. et al. Acetylcholine receptors containing the beta2 subunit are involved in the reinforcing properties of nicotine. *Nature* **391**, 173-177 (1998).
47. Marubio, L. M. et al. Reduced antinociception in mice lacking neuronal nicotinic receptor subunits. *Nature* **398**, 805-810 (1999).
48. Benowitz, N. L. Pharmacology of nicotine: addiction and therapeutics. *Ann. Rev. Pharm.* **36**, 597-613 (1996).
49. Dani, J. A. and Heinemann, S. Molecular and cellular aspects of nicotine abuse. *Neuron* **16**, 905-908 (1996).
50. ChavezNoriega, L. E. et al. Pharmacological characterization of recombinant human neuronal nicotinic acetylcholine receptors h alpha 2 beta 2, h alpha 2 beta 4, h alpha 3 beta 2, h alpha 3 beta 4, h alpha 4 beta 2, h alpha 4 beta 4 and h alpha 7 expressed in *Xenopus* oocytes. *J. Pharm. Exp. Therapeut.* **280**, 346-356 (1997).
51. Papke, R. L. and Heinemann, S. F. Partial Agonist Properties of Cytisine on Neuronal Nicotinic Receptors Containing the Beta-2 Subunit. *Mol. Pharm.* **45**, 142-149 (1994).
52. Spang, J. E. et al. Chemical modification of epibatidine causes a switch from agonist to antagonist and modifies its selectivity for neuronal nicotinic acetylcholine receptors. *Chem. Biol.* **7**, 545-555 (2000).
53. Truong, A. et al. Pharmacological differences between immunoisolated native brain and heterologously expressed rat alpha 4 beta 2 nicotinic receptors. *Mol. Brain Res.* **96**, 68-76 (2001).
54. Gale, M., Tan, S. L. and Katze, M. G. Translational control of viral gene expression in eukaryotes. *Microbiol. Mol. Bio. Rev.* **64**, 239-248 (2000).
55. Hann, L. E., Webb, A. C., Cai, J. M. and Gehrke, L. Identification of a competitive translation determinant in the 3' untranslated region of alfalfa mosaic virus coat protein mRNA. *Mol. Cell. Biol.* **17**, 2005-2013 (1997).
56. Shih, T. M., Smith, R. D., Toro, L. and Goldin, A. L. High-level expression and detection of ion channels in *Xenopus* oocytes. *Meth. Enz.* **293**, 529-556 (1998).
57. Nicke, A. et al. P2X(1) and P2X(3) receptors form stable trimers: a novel structural motif of ligand-gated ion channels. *EMBO J.* **17**, 3016-3028 (1998).

58. Wischmeyer, E., Doring, F. and Karschin, A. Acute suppression of inwardly rectifying Kir2.1 channels by direct tyrosine kinase phosphorylation. *J. Biol. Chem.* **273**, 34063-34068 (1998).
59. Negrutskii, B. S. and El'skaya, A. V. Eukaryotic translation elongation factor 1 alpha: Structure, expression, functions, and possible role in aminoacyl-tRNA channeling. *Prog. Nucl. Acid Res.* **60**, 47-78 (1998).
60. Dreher, T. W., Uhlenbeck, O. C. and Browning, K. S. Quantitative assessment of EF-1 alpha center dot GTP binding to aminoacyl-tRNAs, aminoacyl-viral RNA, and tRNA shows close correspondence to the RNA binding properties of EF-Tu. *J. Biol. Chem.* **274**, 666-672 (1999).
61. Andersen, G. R., Valente, L., Pedersen, L., Kinzy, T. G. and Nyborg, J. Crystal structures of nucleotide exchange intermediates in the eEF1A-eEF1B alpha complex. *Nature Struct. Biol.* **8**, 531-534 (2001).
62. Vitagliano, L., Masullo, M., Sica, F., Zagari, A. and Bocchini, V. The crystal structure of Sulfolobus solfataricus elongation factor 1 alpha in complex with GDP reveals novel features in nucleotide binding and exchange. *EMBO J.* **20**, 5305-5311 (2001).
63. Deschamps, S. et al. 2 Forms of elongation factor-1-alpha (Ef-1-Alpha O and 42sp50), present in oocytes, but absent in somatic cells of *Xenopus laevis*. *J. Cell Biol.* **114**, 1109-1111 (1991).
64. Frydenberg, J., Poulsen, K., Petersen, A. K. B., Lund, A. and Olesen, O. F. Isolation and characterization of the gene encoding Ef-1-Alpha-O, an Elongation-Factor 1-Alpha expressed during early development of *Xenopus laevis*. *Gene* **109**, 185-192 (1991).
65. Johnson, A. D. and Krieg, P. A. A *Xenopus laevis* gene encoding Ef-1-Alpha-S, the somatic form of Elongation-Factor 1-Alpha - sequence, structure, and identification of regulatory elements required for embryonic transcription. *Dev. Gen.* **17**, 280-290 (1995).
66. Damke, H., Baba, T., Warnock, D. E. and Schmid, S. L. Induction of mutant dynamin specifically blocks endocytic coated vesicle formation. *J. Cell Biol.* **127**, 915-34 (1994).
67. van der Bliek, A. M. et al. Mutations in human dynamin block an intermediate stage in coated vesicle formation. *J. Cell Biol.* **122**, 553-563 (1993).
68. Shimkets, R. A., Lifton, R. P. and Canessa, C. M. The activity of the epithelial sodium channel is regulated by clathrin- mediated endocytosis. *J. Biol. Chem.* **272**, 25537-25541 (1997).
69. Hopf, A., Schreiber, R., Mall, M., Greger, R. and Kunzelmann, K. Cystic fibrosis transmembrane conductance regulator inhibits epithelial Na+ channels carrying Liddle's syndrome mutations. *J. Biol. Chem.* **274**, 13894-13899 (1999).
70. Beggah, A. T. and Geering, K. alpha and beta subunits of Na,K-ATPase interact with BiP and calnexin. *Annal. NY Acad. Sci.* **834**, 537-539 (1997).
71. Ma, D. K. et al. Role of ER export signals in controlling surface potassium channel numbers. *Science* **291**, 316-319 (2001).
72. Luetje, C. W., Piattoni, M. and Patrick, J. Mapping of ligand-binding sites of neuronal nicotinic acetylcholine-receptors using chimeric alpha-subunits. *Mol. Pharm.* **44**, 657-666 (1993).
73. Hohsaka, T., Ashizuka, Y., Taira, H., Murakami, H. and Sisido, M. Incorporation of nonnatural amino acids into proteins by using various four-base codons in an *Escherichia coli in vitro* translation system. *Biochemistry* **40**, 11060-11064 (2001).
74. Francis, M. M., Cheng, E. Y., Weiland, G. A. and Oswald, R. E. Specific activation pf the alpha 7 nicotinic acetylcholine receptor by a quaternary analog of cocaine. *Mol. Pharm.* **60**, 71-79 (2001).
75. Nowak, M. W. et al. *In vivo* incorporation of unnatural amino acids into ion channels in *Xenopus* oocyte expression system. *Meth. Enz.* **293**, 504-529 (1998).
76. Li, L. T. et al. The tethered agonist approach to mapping ion channel proteins toward a structural model for the agonist binding site of the nicotinic acetylcholine receptor. *Chem. Biol.* **8**, 47-58 (2001).
77. Davies, P. A. et al. The 5-HT_{3B} subunit is a major determinant of serotonin-receptor function. *Nature* **397**, 359-363 (1999).
78. Sisido, M. and Hohsaka, T. Introduction of specialty functions by the position-specific incorporation of nonnatural amino acids into proteins through four-base codon/anticodon pairs. *App. Microbiol. Biotech.* **57**, 274-281 (2001).
79. Nakamura, Y., Gojobori, T. and Ikemura, T. Codon usage tabulated from international DNA sequence databases: status for the year 2000. *Nuc. Acids Res.* **28**, 292-292 (2000).
80. Saks, M. E. et al. An engineered *Tetrahymena* tRNA(Gln) for in vivo incorporation of unnatural amino acids into proteins by nonsense suppression. *J. Biol. Chem.* **271**, 23169-23175 (1996).

81. Sisido, M. and Hohsaka, T. Extension of protein functions by the incorporation of nonnatural amino acids. *Bull. Chem. Soc. Japan* **72**, 1409-1425 (1999).